



# Quantifying flood-water impacts on a lake water budget via volume-dependent transient stable isotope mass balance

Janie Masse-Dufresne<sup>1</sup>, Florent Barbecot<sup>2</sup>, Paul Baudron<sup>1,3</sup> and John Gibson<sup>4,5</sup>

<sup>1</sup>Polytechnique Montréal, Department of Civil, Geological and Mining Engineering, Montreal, QC H3T 1J4, Canada

5 <sup>2</sup>Geotop-UQAM, Department of Earth and Atmospheric Sciences, Montreal, QC H2X 3Y7, Canada

<sup>3</sup>Institut de Recherche pour le Développement, UMR G-EAU, 34090 Montpellier, France

<sup>4</sup>Alberta Innovates Technology Futures, 3-4476 Markham Street, Victoria, BC V8Z 7X8, Canada

<sup>5</sup>University of Victoria, Department of Geography, Victoria, BC V8W 3R4, Canada

*Correspondence to:* Janie Masse-Dufresne (janie.masse-dufresne@polymtl.ca)

10 **Abstract.** Interactions between groundwater and surface water are often overlooked in lake water budgets, even though  
groundwater can significantly contribute to the total annual water inputs to a lake. Isotope mass balance models have seen  
significant developments in the last decade for assessing the spatial and temporal variability of hydrological processes in  
lakes but are generally applied assuming steady-state. While this assumption is generally acceptable for long-term water  
balances of large lakes, it may be less appropriate for lakes which undergo strong seasonality of hydrological processes and  
15 meteorological conditions. In this study, a volume-dependent transient isotopic mass balance model was developed for an  
artificial lake (named Lake A) in Canada, and in a context where direct measurement of surface water fluxes is difficult, if  
not impossible. This lake typically receives important inputs of flood-water during the spring freshet period, as a hydraulic  
connection with a large watershed establishes each year. Quantification of the water fluxes to Lake A allowed to highlight  
the impacts of flood-water inputs over the annual water budget. The isotopic mass balance model revealed that groundwater  
20 and surface water inputs respectively account for 71 % and 28 % of the total annual water inputs to Lake A, which  
demonstrates its dependence on groundwater. An important part of these groundwater inputs is likely to correspond to flood-  
derived surface water due to bank storage. On an annual timescale, Lake A was found to be resilient to surface water  
pollution and sensitive to groundwater quantity and quality changes. There is however a likelihood that the resilience to  
surface water pollution is lower from April to August, as important water inputs originating from Lake DM contribute to the  
25 water balance via direct and indirect inputs (i.e., from bank storage). This suggests that the surface water fluxes between  
Lake DM and Lake A did not only have an impact on the dynamic of Lake A during springtime but also significantly  
influenced the long-term dynamics of Lake A. These findings can help anticipating the impacts of variation in the intensity  
and/or duration of future flooding events on lakes' water quality. From a more global perspective, this knowledge is useful  
for establishing regional-scale management strategies for maintaining water quality at flood-affected lakes in a context of  
30 land-use and climate changes.



## 1 Introduction

Lakes are complex ecosystems which play valuable economic, social and environmental roles within the watershed (Kløve et al., 2011). In fact, lacustrine ecosystems can provide a number of benefits and services, such as biodiversity, water supply, recreation and tourism, fisheries and sequestration of nutrients (Schallenberg et al., 2013). The actual outcome of these ecosystem services often depends on the water quality of the lake (Mueller et al., 2016). Globally, the quantity and quality of groundwater and surface water resources are known to be affected by land-use (Lerner and Harris, 2009; Cunha et al., 2016; Scanlon et al., 2005) and climate changes (Delpla et al., 2009). As both groundwater and surface water contribute to lake water balances (Rosenberry et al., 2015), changes that affect the process or the surface/groundwater apportionment can potentially modify or threaten lake water quality (Jeppesen et al., 2014). As a consequence, accurate estimation of the inflow and outflow fluxes of groundwater and surface water to a lake have been argued as prerequisite to effective management at the watershed scale (Brooks et al., 2014). Understanding the relative importance of the hydrological processes in lakes can also help to depict the vulnerability and/or resilience of a lake to pollution (Kløve et al., 2011) as well as to invasive species (Walsh et al., 2016).

Over the past few decades, significant developments have been made in application of isotope mass balance models for assessing the spatial and temporal variability of hydrological processes in lakes; most notably, the quantification of groundwater, surface water and evaporative fluxes (Stets et al., 2010; Arnoux et al., 2017a; Bocanegra et al., 2013; Sacks et al., 2014; Gibson et al., 2016). Isotope balance models have also been demonstrated to be useful for quantifying the relative importance of snowmelt water and/or flood-water inputs on the water balance of lakes (Turner et al., 2010; Brock et al., 2007). Most isotope mass balance models are developed assuming constant lake water volume. While this assumption is generally acceptable for long-term water balances of large lakes (Gibson et al., 2015), it may be less appropriate for lakes which undergo strong seasonality of hydrological processes and meteorological conditions (Gibson, 2002).

The main purpose of this study was initially to expand our understanding of flood-affected lake dynamics in the context of a seasonal climate. To do so, we developed a volume-dependent transient isotopic mass balance model and applied it to predict the daily isotopic response of an artificial lake in Canada that is ephemerally connected to a 150,000 km<sup>2</sup> watershed during spring freshet and other periods of flooding. During flooding events, the surficial water fluxes towards the study lake are not constrained in a river or canal but occur over a 1 km long area. In this context, direct measurement of surficial fluxes (e.g., river stage) is difficult, if not impossible, while an isotope mass balance can be applied efficiently considering the heavy-isotope marked flood-water. The democratization of isotope mass balances in Quebec province could be useful to quantify the importance of hydrologic connectivity during flooding events at the watershed scale.

A previous study by Zimmermann (1979) similarly used a transient isotope balance to estimate groundwater inflow and outflow, evaporation, and residence times for two young artificial groundwater lakes near Heidelberg, Germany, although these lakes had no surface water connections, and volumetric changes were considered negligible. Zimmermann (1979) showed that the lakes were actively exchanging with groundwater, which controlled the long-term rate of isotopic



enrichment to isotopic steady state, but the lakes also responded to seasonal cycling in the magnitude of water balance processes. While informative, Zimmermann (1979) did not attempt to build a predictive isotope mass balance model, but rather used a best-fit approach to obtain a solitary long-term estimate of water balance partitioning for each lake. Petermann et al. (2018) also constrained groundwater connectivity for an artificial lake near Leipzig, Germany, with no surface inlet nor outlet. By comparing groundwater inflow rates obtained via stable isotope and radon mass balances on a monthly time-step, Petermann et al. (2018) highlighted the need to consider seasonal variability when conducting lake water budget studies.

Our approach builds on that of Zimmermann (1979) and Petermann et al. (2018), developing a predictive model of both atmospheric and water balance controls on isotopic enrichment, and accounting for volumetric changes on a daily time step. Incorporation of volumetric changes was considered necessary in this application as it spanned an historical flooding event, which led to rapid volume changes in the lake, which was then followed by a steady progression of lake volume increase over a period of 5 months. Quantification of flood-water inputs was achieved by adjusting minimum and maximum values for surface water and groundwater outflows from the lake as a best-fit to the observed lake isotopic compositions. A sensitivity analysis was conducted in order to evaluate and discuss the impact of the uncertainties of the main input parameters and assumptions. By comparing the relative importance of the hydrological processes, we discuss the resilience of our study lake, Lake A, to surface water pollution as well as its sensitivity to groundwater changes.

## 2. Study site

### 2.1 Lake A and Lake DM

Located in southern Quebec, Canada, Lake A is a small artificial lake created by sand dredging activities with a maximum observed depth of 20 m (Fig. 1a). The lake constitutes the main water resource for a bank filtration system (Masse-Dufresne et al., 2019) which is designed to supply drinking water for up to 18,000 people (Ageos, 2010). The lake volume ( $4.70 \times 10^6 \text{ m}^3$ ) was estimated based on its surface area ( $2.79 \times 10^5 \text{ m}^2$  in October 2016, measured on *Google Earth Pro*), maximum observed depth, and assuming lake bed slopes of 25 degrees (Holtz and Kovacs, 1981). A discussion concerning the impact of uncertainty regarding the lake geometry on the model calculation is provided in Sect. 4.3. The lake was excavated within alluvial sands which were deposited in a paleo valley carved into the Champlain Sea Clays (Ageos, 2010). Lake A receives inflow from a small stream (S1) with a mean and maximum annual discharge of  $0.32 \text{ m}^3 \text{ s}^{-1}$  and  $1.19 \text{ m}^3 \text{ s}^{-1}$ , respectively. Maximum discharge typically occurs during the month of April as it drains snowmelt water from a small watershed ( $14.4 \text{ km}^2$ ) (Centre d'Expertise Hydrique du Québec, 2019), whereas low to no flow is recorded during the remainder of the hydrological year. A single outlet stream (S2) allows water to exit Lake A and flow towards Lake DM. The flow direction at S2 can be temporally reversed (Fig. 1b) and allows for surface water inputs from Lake DM to Lake A at times when the water level of Lake DM exceeds that of Lake A above the topographic threshold of 22.12 m.a.s.l. (Ageos, 2010). This process typically occurs during springtime (from April to May) and, less frequently, during autumn (from October to December) and results from snowpack melting and/or abundant precipitation input over the Lake DM watershed.



Significantly, Lake DM (Deux-Montagnes) is the receiving waters for the Ottawa River, which drains a large watershed of approximately 150,000 km<sup>2</sup> (MDDELCC, 2015) and in turn drains via the St. Lawrence River (Fig. 1a). Surface sediments between Lake A and Lake DM (Fig. 1b) are only few meters thick and are overlying the Champlain marine clays, which have poor hydraulic conductivity. Hence, it is likely that no or very limited subsurface hydraulic connection between Lake A and Lake DM exist.

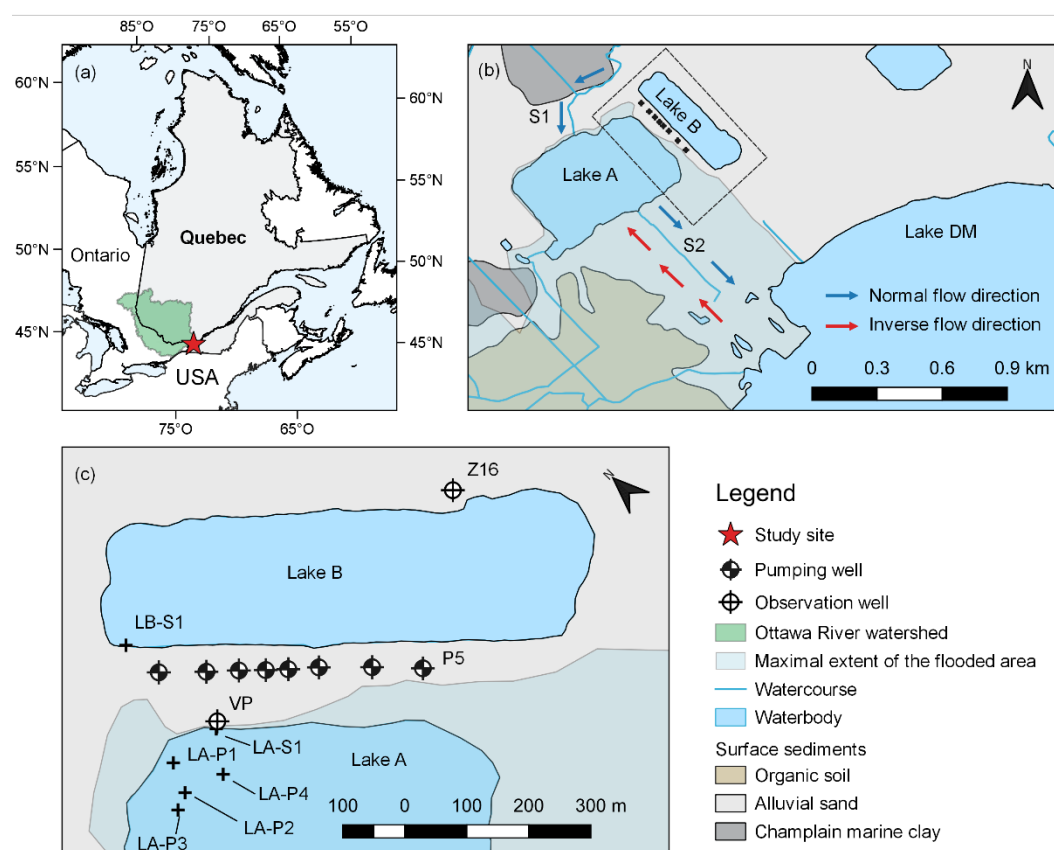


**Figure 1.** (a) Location of the study site and Ottawa River watershed, (b) schematic representation of the hydrogeological context and location of Lake A, Lake B and Lake DM, and (c) location of monitoring and sampling points. LA-S1 and LB-S1 are surface water sampling points at Lake A and Lake B, respectively. LA-P1 to LA-P4 correspond to vertical profile sampling locations at Lake A. Monitoring of the water levels was conducted at pumping well P5 and observation well VP. The maps were created based on open access Geographic Information System (GIS) data. Canada's provinces boundary files were obtained from Statistics Canada © and USA Cartographic Boundary Files were retrieved from the United States Census Bureau ©. Hydrological data (lakes, streams and watershed) was sourced from the Nation Hydro Network – NHN – GeoBase Series and provided by the Strategic Policy and Results Sector of Natural Resources Canada ©. The flood extent products are derived from RADARSAT-2 images with a system developed and operated by the Strategic Policy and Results Sector of Natural Resources Canada ©. The surface sediments data correspond to “Géologie du quaternaire - Jeux de données géographiques - Zones morphosédimentologiques” and are available from Ministère de l'Énergie et des Ressources naturelles; Secteur de l'énergie et des mines – Direction de l'information géologique du Québec ©.



## 2.2 Hydrodynamics of the spring freshet period

Figure 2 illustrates the temporal evolution of the mean daily water level at Lake DM, Lake A, observation well VP and pumping well P5. All water levels are reported relative to a reference water levels measured on February 9, 2017 (i.e., the starting date of the isotopic mass balance). As explained above, water level of Lake DM typically rises during springtime due to snowpack melting over Ottawa River watershed (Centre d'Expertise Hydrique du Québec, 2017). In 2017, rapid water level rise at Lake DM occurred in late February, early April and early May at rates of approximately  $0.11 \text{ m d}^{-1}$ ,  $0.19 \text{ m d}^{-1}$  and  $0.16 \text{ m d}^{-1}$ , respectively. A historical maximum water level (i.e., 24.77 m.a.s.l.) was reached on May 8, 2017, resulting in a net water level rise of 2.72 m compared to early February. Figure 1b-c shows the maximum extent of the flooded area (on May 8, 2017) between Lake DM and Lake A.

Water level monitoring at observation well VP was conducted from April to July 2017, whereas Lake A water level monitoring could only be initiated in late April (due to the presence of an ice-cover). The relative water level variations at all observation points (i.e., Lake A, observation well VP and pumping well P5) are synchronous with those of Lake DM (Fig. 2) from late February to late July 2017. Moreover, the water levels of Lake DM and Lake A were similar or equal for the observed period. Considering this, and a visible hydraulic connection between the water bodies, it becomes clear that Lake DM was controlling the surface water level of Lake A and, consequently, the water table elevation at observation well VP and pumping well P5 during this period. We noted that the elevation of the natural threshold (i.e., 22.12 m.a.s.l.) was exceeded by Lake DM from February 23, 2017 to late July 2017, allowing surface water exchanges between Lake DM and Lake A. Note that pumping well P5 was only occasionally pumping (i.e., few hours per month) during the study period. Hence, the represented evolution of the water level for P5 in Fig. 2 is not affected by drawdown.

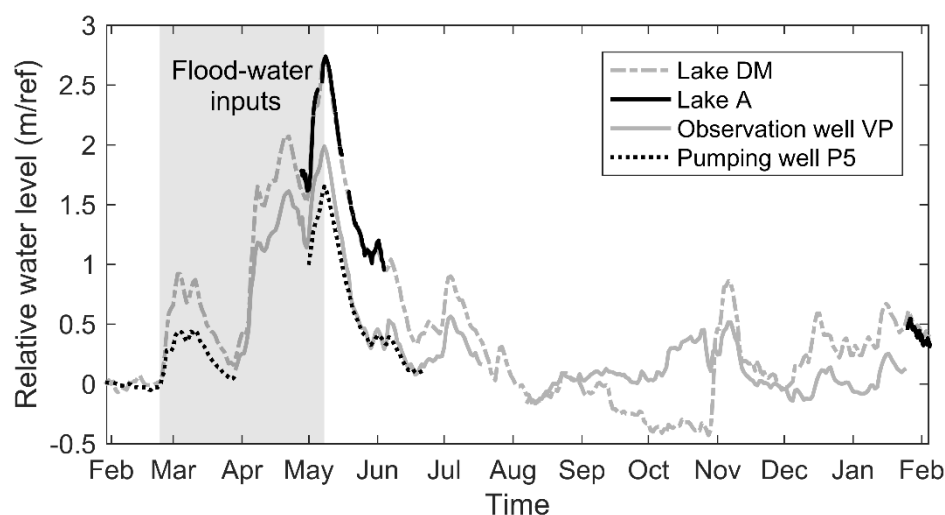


Figure 2. Relative water levels at Lake DM, Lake A, observation well VP and pumping well P5 from February 9, 2017 to January 25, 2018. The grey shaded area corresponds to the flood-water inputs period.



### 3 Methods

#### 3.1 Field measurements

Level loggers (Divers®; TD-Diver and CTD-Diver) were used to measure water levels at Lake A and observation well VP. Water levels were recorded with a 15-minute time step starting on April 17, 2017 and March 29, 2017 at Lake A and VP respectively. Note that water levels in Lake A were not continuously recorded after June 3, 2017 due to a logger failure. Mean daily water levels at Lake DM were retrieved with permission from the *Centre d'Expertise Hydrique du Québec* database (Centre d'Expertise Hydrique du Québec, 2017). Meteorological data from Mirabel International Airport station (45.68 °N, -74.04 °E) were used for further computations and were retrieved from Environment and Climate Change Canada database (available online at weatherstats.ca). Daily precipitation and solar radiation data were retrieved from two nearby stations, namely Sainte-Anne-de-Bellevue (45.43 °N, -73.93 °E) and Montreal International Airport (45.47 °N, -73.75 °E), as these parameters were not available at the closest station.

#### 3.2 Water sampling and analytical techniques

Physico-chemical parameters, including temperature, electrical conductivity, pH and redox potential, and water sampling were measured in Lake A close to the surface near the lake edge on a weekly to monthly basis using a multiparameter probe (YSI Pro Plus 6051030 and Pro Series pH/ORP/ISE and Conductivity Field Cable 6051030-1, YSI Incorporated, Yellow Springs, OH, USA). Additional field campaigns were conducted on February 9, 2017, August 17, 2017 and January 25, 2018 in order to perform vertical profile measurements and water sampling at various depths (e.g. 2 m, 4 m, 8 m, 12 m and 15 m). Flood-water was also sampled on April 19, 2017 and May 10, 2017.

Water samples were analyzed for major ions, alkalinity and stable isotopic compositions of water ( $\delta^{18}\text{O}$  and  $\delta^2\text{H}$ ). Water was filtered in the field using 0.45  $\mu\text{m}$  hydrophilic polyvinylidene fluoride (PVDF) membranes (Millex-HV, Millipore, Burlington, MA, USA) prior to sampling for major ions and alkalinity. During December to March, cold weather prevented field filtration, so this procedure was performed in the laboratory on the same day. All samples were collected in 50-ml polypropylene containers and kept refrigerated at 4 °C during transport and until analysis, except for stable isotope composition which were stored at room temperature. Major ions were analyzed within 48 h via ionic chromatography (ICS 5000 AS-DP Dionex Thermo Fisher Scientific, Saint-Laurent, QC, Canada) at Polytechnique Montreal (Montreal, Quebec). The limit of detection (LOD) was 0.2 mg/L for all major ions. Bicarbonate concentrations were derived from alkalinity, which was measured manually in the laboratory according to the Gran method (Gran, 1952) at Polytechnique Montreal (Montreal, Quebec). On samples with measured alkalinity ( $n = 12$ ), the ionic balance errors were all below 8 %. The mean and median ionic balance errors were 1 %. Stable isotopes of water were measured with a Water Isotope Analyser with off-axis integrated cavity output spectroscopy (LGR-T-LWIA-45-EP, Los Gatos Research, San Jose, CA, USA) at Geotop-UQAM (Montreal, Quebec). Isotopic data were corrected using three internal reference standards ( $\delta^{18}\text{O} = -6.71 \text{ ‰}$ ,  $-4.31 \text{ ‰}$



and -20.31 ‰;  $\delta^{17}\text{O} = -7.23$  ‰, -2.31 ‰ and -19.96 ‰;  $\delta^2\text{H} = -51.0$  ‰, -25.19 ‰ and -155.40 ‰) which are calibrated on the VSMOW-SLAP scale. The analytical uncertainty ( $1\sigma$ ) is 0.15 ‰ and 1 ‰ for  $\delta^{18}\text{O}$  and  $\delta^2\text{H}$ , respectively.

### 3.3 Stable isotope mass balance

170 The water and stable isotope mass balance of a well-mixed lake can be described, respectively as Eq. (1) and Eq. (2):

$$\frac{dV}{dt} = I - E - Q \quad (1)$$

$$V \frac{d\delta_L}{dt} + \delta_L \frac{dV}{dt} = I\delta_I - E\delta_E - Q\delta_Q \quad (2)$$

where  $V$  is the lake volume,  $t$  is time,  $I$  is the instantaneous inflow,  $E$  is evaporation,  $Q$  is the instantaneous outflow.  $I$  correspond to the sum of surface water inflow ( $I_S$ ), groundwater inflow ( $I_G$ ) and precipitations ( $P$ ). Similarly,  $Q$  is the sum of surface water outflow ( $Q_S$ ) and groundwater outflow ( $Q_G$ ).  $\delta_L$ ,  $\delta_I$ ,  $\delta_E$  and  $\delta_Q$  are the isotopic compositions of the lake, the inflow, evaporative and outflow fluxes respectively. Note that  $\delta_Q$  is assumed equal to  $\delta_L$  as for well-mixed lake water conditions. The application of Eq. (1) and Eq. (2) for both  $\delta^{18}\text{O}$  and  $\delta^2\text{H}$  is valid during the ice-free period and also assumes constant density of water (Gibson, 2002).

180 The isotopic composition of the evaporating moisture ( $\delta_E$ ) is estimated based on the Craig and Gordon (1965) model and, as described by Gonfiantini (1986), is:

$$\delta_E = \frac{\frac{(\delta_L - \epsilon^+)}{\alpha^+} - h\delta_A - \epsilon_K}{1 - h + 10^{-3}\epsilon_K} \text{ (‰)} \quad (3)$$

where  $h$  is the relative humidity normalized to water surface temperature (in decimal fraction),  $\delta_A$  is the isotopic composition of atmospheric moisture (described later on),  $\epsilon^+$  is the equilibrium isotopic separation and  $\epsilon_K$  is the kinetic isotopic separation, with  $\epsilon^+ = (\alpha^+ - 1)10^3$  and  $\epsilon_K = \theta * C_K(1 - h)$ .  $\alpha^+$  is the equilibrium isotopic fractionation,  $\theta$  is a transport resistance parameter and  $C_K$  is the ratio of molecular diffusivities of the heavy and light molecules.  $\theta$  is expected to be close to 1 for small lakes (Gibson et al., 2015) and  $C_K$  is typically fixed at 14.2 ‰ and 12.5 ‰ for  $\delta^{18}\text{O}$  and  $\delta^2\text{H}$  respectively in lake studies as these values represent fully turbulent wind conditions (Horita et al., 2008). Experimental values for  $\alpha^+$  were used (Horita and Wesolowski, 1994):

$$\alpha^+(\text{}^{18}\text{O}) = \exp \left[ -\frac{7.685}{10^3} + \frac{6.7123}{(T+273.15)} - \frac{16666.4}{(T+273.15)^2} + \frac{350410}{(T+273.15)^3} \right] \quad (4a)$$

$$190 \quad \alpha^+(\text{}^2\text{H}) = \exp \left[ 1158.8 \left( \frac{(T+273.15)^3}{10^{12}} \right) + 1620.1 \left( \frac{(T+273.15)^2}{10^9} \right) + 794.84 \left( \frac{(T+273.15)}{10^6} \right) - \frac{161.04}{10^3} + \frac{2999200}{(T+273.15)^3} \right] \quad (4b)$$

where  $T$  is the temperature (°C) of water surface.

The isotopic composition of atmospheric moisture ( $\delta_A$ ) was estimated using the partial equilibrium model of Gibson et al. (2015):





$$\delta_A = \frac{\delta_P - k\epsilon^+}{1 + 10^{-3} \cdot k\epsilon^+} \quad (5)$$

195 where  $\delta_P$  is the isotopic composition of precipitation and  $k$  is a seasonality factor, ranging from about 0.5 to 1. The  $k$  value is selected to provide a best-fit between the measured and modelled local evaporation line. Note that  $\delta_P$  and monthly exchange parameters ( $\epsilon^+$ ,  $\alpha^+$  and  $\epsilon_K$ ) were evaporation flux-weighted based on daily evaporation records from the site. These parameters were considered constant over each one-month period and used in the model for the calculation of  $\delta_A$  and  $\delta_E$ . In this study, the lake volume change over time is significant and, thus, a volume-dependent model is applied assuming well-  
 200 mixed conditions, as described in Gibson (2002). The change in the isotopic composition of the lake with  $f$ , the remaining fraction of lake water, can be expressed as Eq. (6):

$$\delta_L(f) = \delta_S - (\delta_S - \delta_0) f^{\left[\frac{-(1+mX)}{1-X-Y}\right]} \quad (6)$$

where  $X = E/I$  is the fraction of lake water lost by evaporation,  $Y = Q/I$  is the fraction of lake water lost to liquid outflows, and

$$m = \frac{\left(h - 10^{-3} \cdot \left(\epsilon_K + \frac{\epsilon^+}{\alpha^+}\right)\right)}{(1 - h + 10^{-3} \cdot \epsilon_K)} \quad (7)$$

$$\delta_S = \frac{\delta_I + mX\delta^*}{1 + mX} \quad (8)$$

$$\delta^* = \left(h\delta_A + \epsilon_K + \frac{\epsilon^+}{\alpha^+}\right) / \left(h - 10^{-3} \cdot \left(\epsilon_K + \frac{\epsilon^+}{\alpha^+}\right)\right) \quad (9)$$

where  $m$  is the temporal enrichment slope,  $\delta_S$  is the steady-state isotopic composition the lake would attain if  $f$  tends to 0, and  $\delta^*$  is the limiting isotopic composition (Gibson et al., 2015).

A step-wise approach is used to solve Eq. 6, as suggested by (Gibson, 2002). At each time step, recalculation of  $f = V/V_0$  is  
 210 needed, where  $V$  is the residual volume at the end of the time step and  $V_0$  the original volume at the beginning of the time step (or  $V^{t-dt}$ ). Similarly, the initial isotopic composition of the lake ( $\delta_0$ ) corresponds to  $\delta_L^{t-dt}$ . All other parameters are assumed constant over each time step. If  $1 - X - Y$  is equal to zero, Eq. 6 is not valid. In this situation, the lake volume is constant (i.e.  $dV/dt=0$ ) and we solve Eq. (10) (Gibson, 2002):

$$\delta_L = \delta_S - (\delta_S - \delta_0) \exp\left[-(1 + mX) \frac{It}{V}\right] \quad (10)$$

### 215 3.3.1 Water fluxes

The above-mentioned equations are computed on a daily time step to calculate the isotopic composition of the lake ( $\delta_L$ ). Among all the parameters in Eq. (1) and Eq. (2), only surface and groundwater inflows and outflows were not estimated or measured. For well-mixed conditions, the isotopic composition of the surface and groundwater outflows ( $\delta_{Qs}$  and  $\delta_{Qg}$ ) are assumed to be equal to  $\delta_L$ . Hence, no separation of these two fluxes is attempted and they are merged into one variable, i.e.





the non-fractionating outflow ( $Q$ ). Outflow was adjusted to obtain the best fit between the observed and modelled values. The direction and intensity of the water flux at the lake-aquifer interface can be conceptually described by Darcy's Law, which states that the water flux through porous media is dependent on the hydraulic conductivity, the cross-sectional flow area and the hydraulic gradient. Assuming homogenous hydraulic conductivity of the sediments, a water level change at Lake A would only affect the hydraulic gradient between the lake and the aquifer. The variation of the cross-sectional area is negligible, given the significant depth of Lake A (i.e., 20 m) in comparison to the maximum water level change during the flooding event (i.e., 2.7 m). Hence, we assumed that daily minimum and maximum outflow from Lake A occurred at the minimum and maximum water levels, respectively. Outflow fluctuations were derived from water level variations at Lake A using linear interpolation between adjusted daily minimum and maximum outflow. Daily inflow into Lake A was calculated to compensate for the adjusted outflow, as the net water fluxes are required to be equal to the lake's daily volume variation.

As inflows include both surface and groundwater inflows, further assumptions are needed to apportion these contributions. Surface water inflow is set to zero, except for the period of water level rise at Lake A (i.e. from February 23, 2017 to May 8, 2017). During this period, a hydraulic gradient forcing the surface water from Lake A to infiltrate the aquifer would have developed, since Lake A water level was most likely higher than the groundwater table. Thus, when surface inflows into Lake A are contributing to the lake water balance, the groundwater inflows can be neglected and vice versa. It is assumed that the surface water inflows principally originate from Lake DM via S2 (with reversed flow direction, see Sect. 2). Potential surface water inflow from S1 and runoff are not evaluated. The isotopic composition for these two potential inputs is expected to be similar to the flood-water inputs. Moreover, as explained in Sect. 2.2, S1 is typically discharging during springtime, while during the rest of the hydrological year, only negligible or no flow is observed at S1. Hence, these potential inputs are comprised within the daily surface water inflows.

Evaporation was calculated on a daily time step using the Penman evaporation equation, as described in Valiantzas (2006):

$$E_{Penman-48} = \frac{\Delta}{\Delta + \gamma} \cdot \frac{R_n}{\lambda} + \frac{\gamma}{\Delta + \gamma} \cdot \frac{6.43 f(u) D}{\lambda} \quad (11)$$

where  $R_n$  is the net solar radiation ( $\text{MJ m}^{-2} \text{d}^{-1}$ ),  $\Delta$  is the slope of the saturation vapor pressure curve ( $\text{kPa } ^\circ\text{C}^{-1}$ ),  $\gamma$  is the psychrometric coefficient ( $\text{kPa } ^\circ\text{C}^{-1}$ ),  $\lambda$  is the latent heat of vaporization ( $\text{MJ kg}^{-1}$ ),  $f(u)$  is the wind function and  $D$  is the vapor pressure deficit. Various forms of wind function  $f(u)$  have been developed for diverse applications. We opted to use an area-dependent wind function  $f(u)$  and which was developed for land-based meteorological data (McJannet et al., 2012):

$$f(u) = (2.36 + 1.67u)A^{-0.05} \quad (12)$$

where  $u$  is the wind speed ( $\text{m s}^{-1}$ ) measured at 2 m above the ground and  $A$  is the area ( $\text{m}^2$ ) of the lake. Note that evaporation and precipitation fluxes were set to zero during the ice-cover period (i.e. from January 1<sup>st</sup> to March 31, based on meteorological data and field observations).

For comparative purposes, estimation of the daily evaporative fluxes was also conducted with the Linacre-OW equation (Linacre, 1977) and the open-water simplified version of Penman-48 (Valiantzas, 2006). The input parameters for Linacre-



OW equation include latitude (degrees), altitude (m.a.s.l.), mean air temperature ( $^{\circ}\text{C}$ ) and mean dew-point ( $^{\circ}\text{C}$ ). Penman-48 is applied using the simplified open-water version which relies on solar radiation ( $\text{MJ m}^{-2} \text{d}^{-1}$ ), mean, minimum and maximum air temperature ( $^{\circ}\text{C}$ ), relative humidity (%) and wind speed ( $\text{m s}^{-1}$ ). Note that water surface temperature is not  
 255 needed for the application of Linacre-OW and the open-water simplified version of Penman-48. These methods yielded similar evaporation estimates from April to August but underestimated total evaporation by 24 % to 33 % compared to the Penman-48 equation. The discrepancy between the models is restricted to late summer and autumn (see Appendix A, Fig. A1) and is attributed to the difference between the air and water surface temperature.

The water surface temperature was estimated via the equilibrium method presented by de Bruin (1982), since no continuous  
 260 measurements were available. This model is based on the assumption of a well-mixed surface body and was developed from standard land-based weather data. It was tested on two adjacent reservoirs in the Netherlands with average depths of 5 m and 15 m, respectively. In a similar way to de Bruin (1982), we used the 10-day mean values, since we are interested in the annual variations of the water temperature. Moreover, the 10-day mean values were found to better simulate the observed water surface temperature. Differences between the observed and modelled water temperature is typically  $\leq 1^{\circ}\text{C}$ , except in  
 265 July and December where discrepancies up to  $5^{\circ}\text{C}$  were observed (see Appendix B, Fig. B1). This is likely because Lake A develops a thermal stratification over summertime and in wintertime. Potential uncertainties in isotopic mass balance models due to stratification in lakes up to 35 m were previously described and discussed by Gibson et al. (2017) and (Gibson et al., 2019). They reported that sampling methods and lake stratification can lead to volume-dependent bias in the water balance partition. In this study, not accounting fully for thermal stratification will lead overestimation of evaporation fluxes, and  
 270 groundwater exchange will be potentially underestimated.

### 3.3.2 Isotopic framework

The isotopic composition of precipitation, Lake A and flood-water are depicted in Fig. 3. The Local Meteoric Water Line (LMWL) was defined using an ordinary least squares regression (Hughes and Crawford, 2012) using isotope data in precipitation from St-Bruno station IRRES database ( $n = 27$ ; from December 2015 to June 2017). For the study period, the  
 275 isotopic composition of bulk precipitation ( $\delta_P$ ) was available on a biweekly to monthly time-step ( $n = 15$ ) and ranged from -19.19 ‰ to -6.85 ‰ for  $\delta^{18}\text{O}$  and -144 ‰ to -38 ‰ for  $\delta^2\text{H}$ . Interpolation was used to simulate the  $\delta_P$  on a daily-time step. Isotopic compositions of Lake A water samples ( $n = 39$ ) are linearly correlated (see solid blue line) and all plot below the Local Meteoric Water Line (LMWL), which confirms that Lake A is influenced by evaporation. Linear regression of Lake A water samples defines the Local Evaporation Line (LEL), which is  $\delta^2\text{H} = 5.68 (\pm 0.27) * \delta^{18}\text{O} - 12.80 (\pm 2.83)$  ( $R^2 = 0.92$ ).  
 280 Some samples from the surface of Lake A plot below the LEL, likely indicating snowmelt water inputs as noted in previous studies of Canadian lakes (Wolfe et al., 2007). The isotopic composition of the flood-water samples ( $n = 3$ ) are more depleted than Lake A waters (i.e.  $\delta^{18}\text{O}$  from -11.85 ‰ to -11.18 ‰ and  $\delta^2\text{H}$  from -81 ‰ to -78 ‰). They are also linearly correlated and plot along a line ( $\delta^2\text{H} = 5.33 \delta^{18}\text{O} - 18.82$ ) which slope is similar to the LEL, suggesting that flood-water evaporated under same conditions as Lake A water samples. For this reason, we suppose that the isotopic composition of the



285 surface water inflow ( $\delta_{Is}$ ) corresponds to the intersection with the LMWL, i.e., -12.00 ‰ for  $\delta^{18}O$  and -83 ‰ for  $\delta^2H$ . The flood-water isotopic compositions are most likely to reflect the significant contribution from heavy isotope depleted snowmelt waters. Similar isotopic compositions were recorded upstream of Lake DM during the snowmelt period near our study site (i.e., 34 km upstream in the watershed) from 1998 to 2009 (Rosa et al., 2016). It has been argued that the LEL-LMWL intersection is an acceptable proxy for the isotopic composition of the inflowing water to a lake (Gibson et al., 1993; Wolfe et al., 2007; Edwards et al., 2004). Hence, we estimated the isotopic composition of groundwater ( $\delta_G$ ) from the intersection between the St-Bruno LMWL (Barbecot et al., 2019) and Lake A LEL, which corresponds to -11.26 ‰ for  $\delta^{18}O$  and -77 ‰ for  $\delta^2H$ . The isotopic composition of the atmospheric vapour ( $\delta_A$ ) was estimated from Eq.(5) and  $k$  was fixed to 0.5. Finally, the potential impacts of the ice-cover formation and melting were neglected in the isotopic mass balance, as the ice volume is likely to represent only a small fraction (<2 %) of the entire water body. Moreover, flood-water inputs from Lake DM were expected to be much more important and occurring simultaneously with ice-melt during the freshet period.

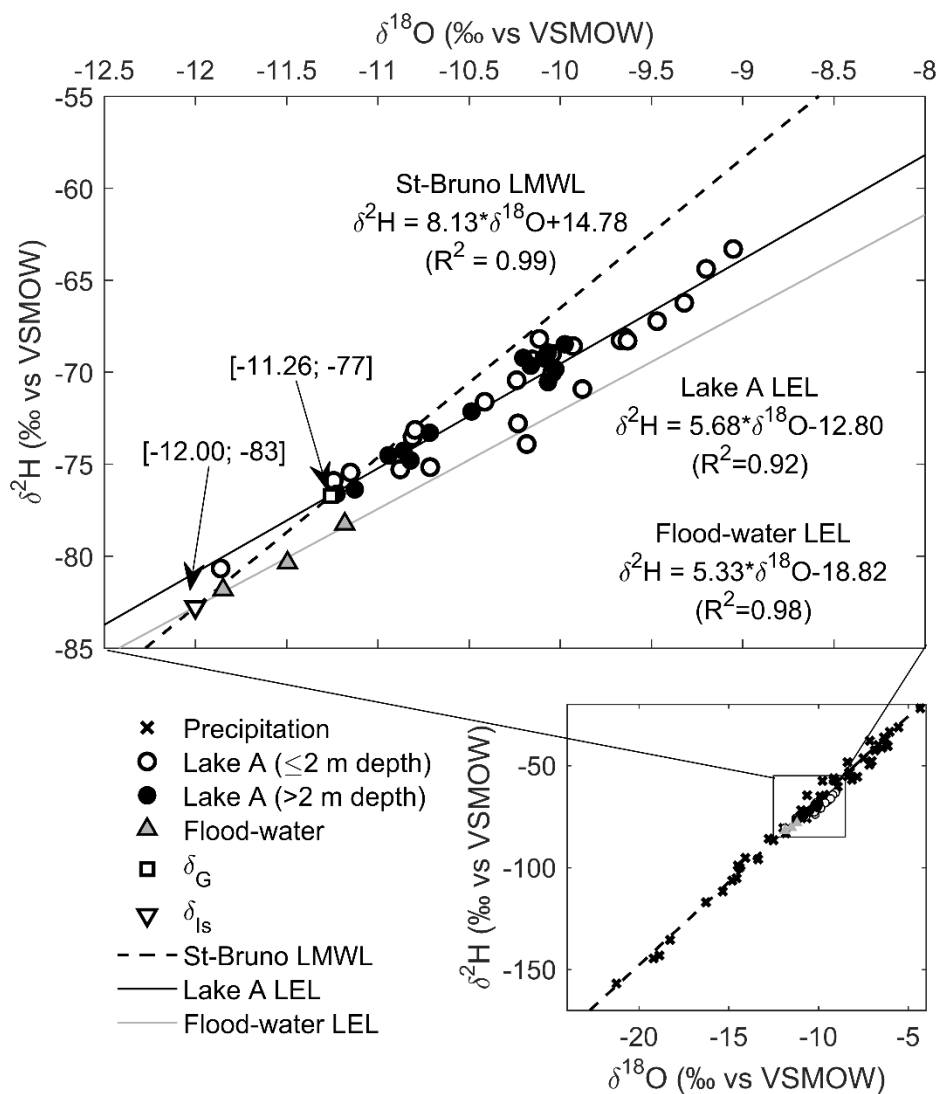


**Figure 3.** Isotopic composition of precipitation, Lake A water, and flood-water from March 2017 to January 2018. Hollow and solid blue circles correspond to samples collected at  $\leq 2$  m and  $> 2$  m depth, respectively. Analytical precision is 0.15‰ and 1‰ at  $1\sigma$  for  $\delta^{18}\text{O}$  and  $\delta^2\text{H}$ . Precipitation data are retrieved from the research infrastructure on groundwater recharge database (Barbecot et al., 2019).



## 4 Results

### 4.1 Deciphering surface and groundwater inputs via stable isotopes of water

305 The temporal evolution of  $\delta^{18}\text{O}$  at the surface ( $\leq 2$  m) and at depth ( $> 2$  m) in Lake A are depicted in Fig. 4. The flood-water ( $\delta_{\text{fs}}$ ) and groundwater ( $\delta_{\text{G}}$ ) isotopic compositions are also included for comparison (see the dotted lines). The spatiotemporal evolution of  $\delta^2\text{H}$  (not shown) was found to be similar that of  $\delta^{18}\text{O}$ . On February 9, 2017, the isotopic composition was ranging between  $-10.24\text{‰}$  and  $-9.97\text{‰}$ , indicating a relatively well-mixed lake. In section 2.2, it was established that significant surface water inputs could have entered Lake A from February 23, 2017 to May 8, 2017 based on the water level

310 variations at Lake A and Lake DM (Fig. 2). In fact, on April 27, 2017, the isotopic composition at the surface of Lake A (i.e.,  $-11.86\text{‰}$ ) was similar to that of flood-water (i.e.,  $-12.00\text{‰}$ ). This may suggest that flood-water was not instantaneously mixed with Lake A water. However, in the study region, the lakes are typically dimictic (Wetzel, 1975; Hutchinson, 1957), i.e., that they experience turnover of the water column in spring and late autumn. Arnoux et al. (2017b) observed that the spring mixing occurs from mid-May to early June at Lake Lacasse (approximately 80 km NW of the study site). Hence,

315 Lake A likely went through a turnover of its water column during the same period. However, this hypothesis is unconfirmed as no vertical profile sampling campaign could be carried during spring due to accessibility issues related to the flooding (i.e., road closures). Hence, the isotopic composition at the surface of Lake A in early May (i.e.,  $-11.24\text{‰}$  to  $-11.15\text{‰}$ ) is deemed to be representative of the entire water column. During summertime, a gradual enrichment of the isotopic composition at the surface of Lake A was observed due to evaporation. Maximum isotopic enrichment (i.e.,  $-9.32\text{‰}$ ) was

320 observed on August 17, 2017. Contrastingly, at depth, the lake water remained isotopically depleted (i.e.,  $-11.23\text{‰}$  to  $-10.94\text{‰}$ ) and more similar to the isotopic composition of groundwater. During autumn, the evaporative fluxes became less important and the isotopic composition Lake A surface water became more depleted. Finally, in late January 2018, the isotopic composition of Lake A was found to be relatively homogenous throughout the water column. This is likely the result of autumnal turnover (Arnoux et al., 2017b). Note that, the isotopic composition is slightly less enriched in heavy isotopes

325 than during the previous winter (i.e.,  $-10.86\text{‰}$  to  $-10.23\text{‰}$ ).

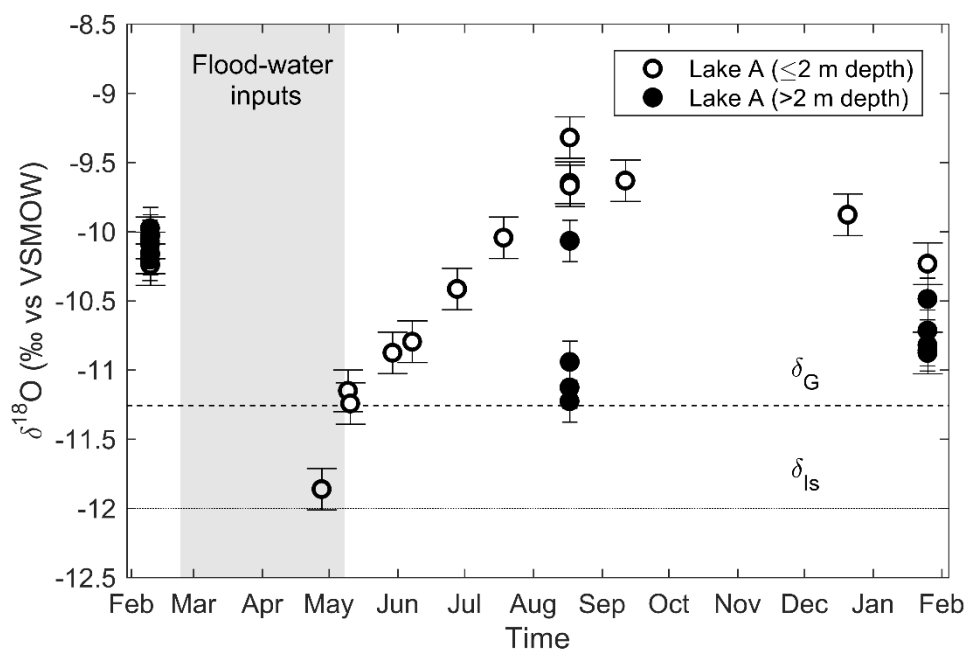


**Figure 4.** Temporal evolution of  $\delta^{18}\text{O}$  at the surface ( $\leq 2$  m) and at depth ( $> 2$  m) in Lake A compared to the isotopic compositions of groundwater ( $\delta_G$ ) and flood-water ( $\delta_{Is}$ ). The grey shaded area corresponds to the flood-water input period.

## 4.2 Quantification of flood-water inputs into Lake A

### 330 4.2.1 Insights from net water fluxes at Lake A

Lake A volume variations are estimated from water level records assuming a constant lake area. When not available, the surface elevation of Lake A is assumed to be equal to the water level at other observation points. Water level of Lake DM is used when hydraulic connection with Lake A is probable. Otherwise, the water table elevation at observation well VP is used (see Sect. 2.2). Figure 5 illustrates the cumulative volume change of Lake A after February 9, 2017 (on the left axis) and daily net water flux (on the right axis) from February 2017 to January 2018.

From February 23, 2017 to May 8, 2017, the relative volume of Lake A is globally increasing, and the net water fluxes are mainly positive (see shaded area in Fig. 5). The maximum volume change of Lake A was  $7.6 \times 10^5 \text{ m}^3$ , which represents 16 % of the lake's initial volume. The maximum net water flux was  $1.2 \times 10^5 \text{ m}^3 \text{ d}^{-1}$ , corresponding to a water level rise of 0.43 m (on April 5, 2017 only). From May 9, 2017 to mid-August 2017, Lake A volume was decreasing, and the daily net water fluxes were mainly negative. On early August 2017, Lake A regained its initial volume. Then, in autumn and winter, the volume of Lake A was oscillating, and the net water fluxes were ranging from  $-6.4 \times 10^4 \text{ m}^3 \text{ d}^{-1}$  to  $5.3 \times 10^4 \text{ m}^3 \text{ d}^{-1}$ . At the end of the study period (i.e., on January 25, 2018), a net volume difference of  $1.5 \times 10^5 \text{ m}^3$  remained at Lake A compared to February 9, 2017.



However, the evolution of Lake A volume and the net water fluxes are not representative of the surface water/groundwater interactions. Since dredged lakes are known to be hydraulically connected with groundwater, the total outflows from Lake A during springtime are likely to be much more important than the net water fluxes.

For that reason, the development of a volume-dependent transient stable isotope mass balance was required to correctly depict the importance of the flood-water inputs on the water mass balance of the lake. The results of this model are presented in the next subsection.

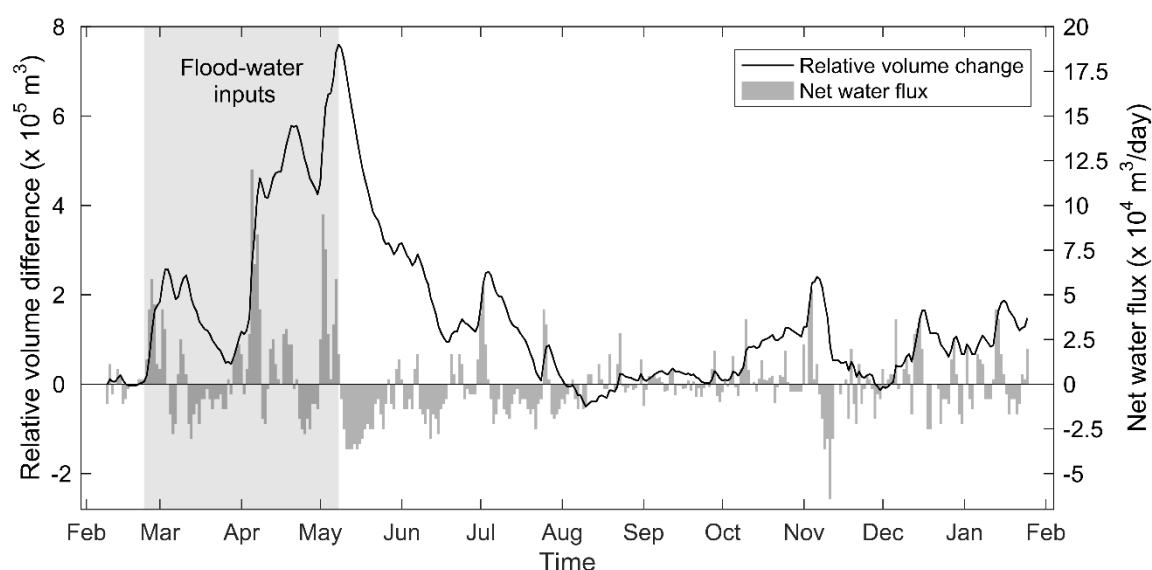


**Figure 5.** Relative volume change of Lake A compared to February 9, 2017 (on the left axis) and the daily net water flux (on the right axis) from February 2017 to January 2018. The grey shaded area corresponds to the flood-water inputs period.

#### 4.2.2 Volume-dependent isotopic mass balance

As described in Sect. 3.3, the isotopic mass balance model was solved iteratively by recalculating  $\delta_L$  on a daily time-step. This model was developed assuming (1) well-mixed conditions and (2) that the outflow fluxes are proportional to the lake's water level. We adjusted minimum and maximum outflow fluxes ( $Q$ ) so that the latter respectively correspond to the minimum and maximum water levels. Three sampling campaigns (i.e., on February 9, 2017, August 17, 2017 and January 25, 2018) were conducted at Lake A in order to collect water samples for isotopic analyses along vertical profiles. The isotope vertical profiles were volume-weighted according to the representative layer for each discrete measurement in order to obtain the observed  $\delta_L$  for each campaign (Table 1). The depth-averaged isotopic composition of the lake on February 9, 2017 (i.e.,  $\delta^{18}\text{O} = -10.15 \text{ ‰}$  and  $\delta^2\text{H} = -70 \text{ ‰}$ ) was used as the initial modelled  $\delta_L$ .





365 **Table 1. Observed depth-averaged (or mean) and standard deviation (std) of isotopic composition of Lake A for the sampling campaigns in February 2017, August 2017 and January 2018 and all samples.**

Date	$\delta^{18}\text{O}$ (‰)		$\delta^2\text{H}$ (‰)	
	depth-averaged	std	depth-averaged	std
Feb 9, 2017	-10.15	0.11	-69.92	0.41
Aug 17, 2017	-10.61	0.82	-73.33	4.41
Jan 25, 2018	-10.70	0.26	-73.70	1.22
All samples (from Feb 9, 2017 to Jan 25, 2018)	-10.32*	0.62	-71.35*	3.69

\* mean

The results of the volume-dependent isotopic mass balance for  $\delta^{18}\text{O}$  and  $\delta^2\text{H}$  are illustrated in Fig. 6. The fitted minimum and maximum  $Q$  from Lake A are  $3.7 \times 10^4 \text{ m}^3 \text{ d}^{-1}$  and  $8.0 \times 10^4 \text{ m}^3 \text{ d}^{-1}$ , respectively. These flows represent water level variations of  $0.13 \text{ m d}^{-1}$  and  $0.29 \text{ m d}^{-1}$ , which is a plausible range for the combination of surface and groundwater outflow processes. From February 23, 2017 to May 8, 2017 (see grey shaded area), hydraulic conditions allowed for surface inputs ( $I_s$ ) from Lake DM to Lake A at a mean rate of  $6.61 \times 10^4 \text{ m}^3 \text{ d}^{-1}$  with a total flood-water volume of  $4.82 \times 10^6 \text{ m}^3$ . The mean outflow rate ( $Q$ ) was  $5.64 \times 10^4 \text{ m}^3 \text{ d}^{-1}$ . The total outflow volume was  $4.12 \times 10^6 \text{ m}^3$ , representing 88 % of the initial lake volume. Then, from May 9, 2017, we considered that these flood-water inputs stopped, as the lake water level started to decrease. As a consequence, the model yielded a gradual enrichment of  $\delta_L$  due to the combined contribution from  $I_G$  and  $E$ . From May 9, 2017 to January 25, 2018, the mean  $I_G$  was  $4.43 \times 10^4 \text{ m}^3 \text{ d}^{-1}$ , which led to a total volume of groundwater  $1.16 \times 10^7 \text{ m}^3$ . For the entire modelled period, a mean annual inflow ( $I$ ) of  $4.86 \times 10^4 \text{ m}^3 \text{ d}^{-1}$  was found to fit the observed  $\delta_L$ . The corresponding mean annual outflow ( $Q$ ) was  $4.77 \times 10^4 \text{ m}^3 \text{ d}^{-1}$ . Overall, the  $\delta^{18}\text{O}$  and  $\delta^2\text{H}$  models were better at reproducing the January and August observed  $\delta_L$ , respectively. This is likely linked to the uncertainties and representativeness of the meteorological data, which is controlling the evaporation rates and to some extent the isotopic fractionation. The development of a multi-layered model, as suggested by Arnoux et al (2017), would be useful to quantify the impact of the lake thermal and isotope stratification on the computed water fluxes. Due to the paucity of the data, it was deemed preferable to develop a simple well-mixed model as a first estimation of the water budget. Further research would be needed to correctly address this question.

### 385 4.3 Sensitivity analysis

A sensitivity analysis was conducted on the input variables of the isotopic mass balance model. For each parameter, we tested two scenarios which delimit the uncertainty for each parameter. First, we tested the sensitivity of the model for  $V + 3 \%$  and  $V - 8 \%$  (i.e., estimated with slopes of  $30^\circ$  and  $20^\circ$ ). Concerning  $\delta_{Is}$   $\delta_G$ , the model was tested for  $\pm 0.5 \%$  for  $\delta^{18}\text{O}$  and  $\pm 4 \%$  for  $\delta^2\text{H}$ , assuming they would both evolve along the LMWL (see Fig. 3). Then, we assessed for the sensitivity of the model to  $\delta_A$ , by fixing the seasonality factor  $k$  at 0.5 and 0.9. Evaporation was computed with  $\pm 20\%$ , whereas the meteorological parameters (i.e., RH, T, U, P and  $R_s$ ) were tested for  $\pm 10\%$ . Since  $E$  and  $\delta_A$  are dependent on the

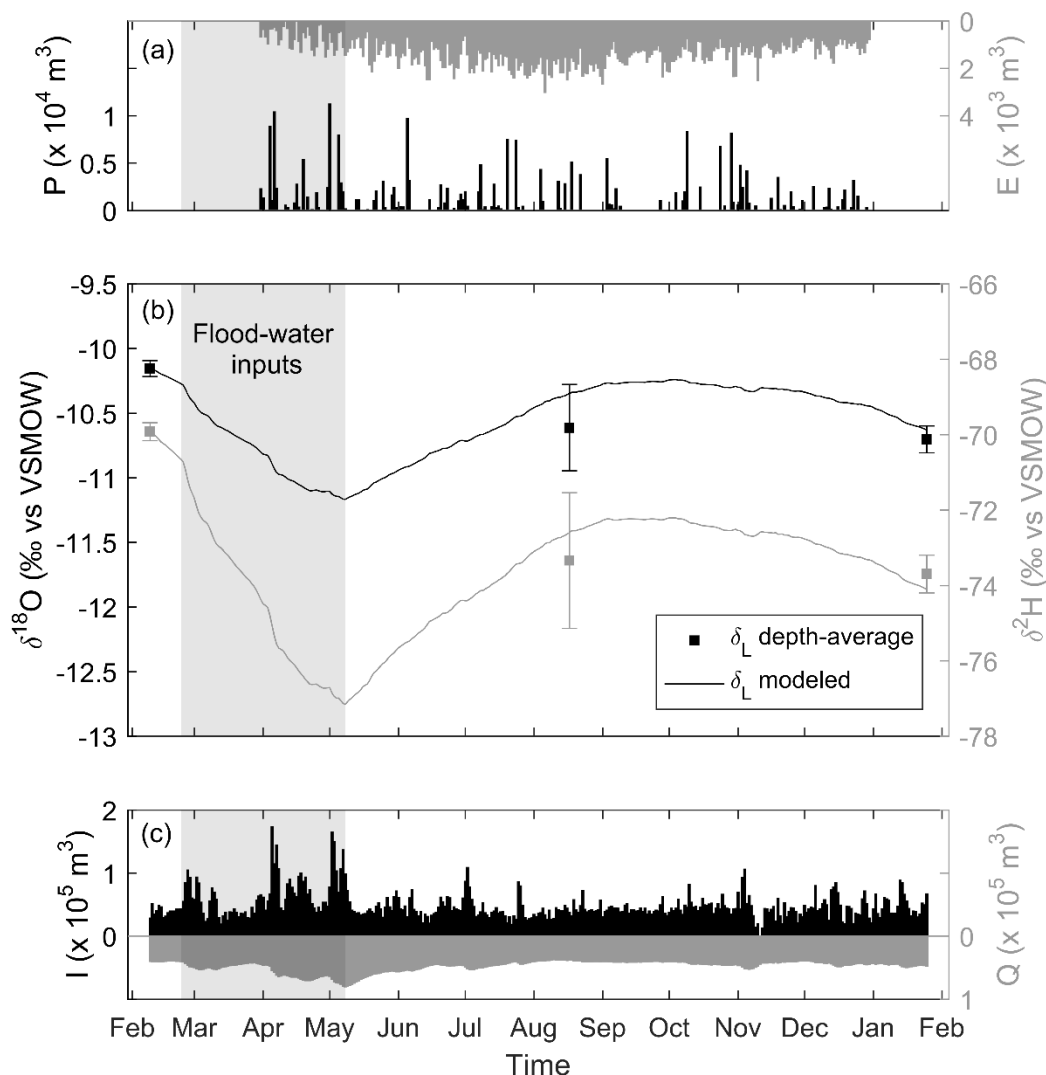


**Figure 6.** Daily precipitation ( $P$ ) and evaporative fluxes ( $E$ ) normalized to Lake A surface (a), measured and modelled depth-average isotopic composition of the lake ( $\delta_L$ ) for  $\delta^{18}\text{O}$  and  $\delta^2\text{H}$  (b) and the daily estimated water inputs ( $I$ ) and adjusted water output ( $Q$ ) from February 9, 2017 to January 25, 2018 (c). The grey shaded area corresponds to the flood-water inputs period. The error bars correspond to the standard error on the samples for each campaign.



**Table 2. Sensitivity analysis on the input parameters of the isotopic mass balance model. Q is the output flux from Lake A, I the input flux and  $t_f$  the mean flushing time by groundwater.**

Scenario		Maximum Q (x 10 <sup>4</sup> m <sup>3</sup> d <sup>-1</sup> )	Minimum Q (x 10 <sup>4</sup> m <sup>3</sup> d <sup>-1</sup> )	Mean Q		Mean I		Tf = V/I <sub>G</sub> (days)
				Flooding	Annual	Flooding	Annual	
				(x 10 <sup>4</sup> m <sup>3</sup> d <sup>-1</sup> )		(x 10 <sup>4</sup> m <sup>3</sup> d <sup>-1</sup> )		
A	Reference	8,0	3,7	5,64	4,77	6,61	4,86	135
A01	V + 3% (slope 30°)	8,0	3,7	5,64	4,77	6,61	4,86	140
A02	V - 8% (slope 20°)	7,8	3,7	5,55	4,72	6,51	4,81	129
A03	δ <sub>Is</sub> <sup>18</sup> O + 0.5 ‰ δ <sub>Is</sub> <sup>2</sup> H + 4 ‰	25,0	1,0	11,82	6,99	12,79	7,08	106
A04	δ <sub>Is</sub> <sup>18</sup> O - 0.5 ‰ δ <sub>Is</sub> <sup>2</sup> H - 4 ‰	4,3	4,2	4,25	4,22	5,21	4,31	150
A05	δ <sub>G</sub> <sup>18</sup> O + 0.5 ‰ δ <sub>G</sub> <sup>2</sup> H + 4 ‰	Not possible to fit data						
A06	δ <sub>G</sub> <sup>18</sup> O - 0.5 ‰ δ <sub>G</sub> <sup>2</sup> H - 4 ‰	10,0	1,0	5,06	3,25	6,02	3,34	189
A07	δ <sub>A</sub> minimum	Not possible to fit data						
A08	δ <sub>A</sub> maximum	8,0	4,0	5,80	5,00	6,77	5,09	148
A09	E + 20%	8,0	4,8	6,24	5,60	7,22	5,72	110
A10	E - 20%	8,0	2,7	5,09	4,02	6,05	4,09	156
A11	RH + 10%	Negligible change						
A12	RH - 10%							
A13	T + 10%	8,0	3,9	5,75	4,92	6,71	5,01	130
A14	T - 10%	8,0	3,5	5,53	4,62	6,50	4,71	140
A15	U + 10%	8,0	3,9	5,75	4,92	6,72	5,01	130
A16	U - 10%	8,0	3,6	5,58	4,70	6,55	4,78	137
A17	P + 10%	Negligible change						
A18	P - 10%							
A19	T <sub>w</sub> = T <sub>air</sub>	10,0	2,9	6,10	4,67	7,07	4,73	145
A20	R <sub>S</sub> + 10%	8,0	3,9	5,75	4,92	6,72	5,02	125
A21	R <sub>S</sub> - 10%	8,0	3,6	5,58	4,70	6,55	4,78	146
A22	LMWL (PWLSR method)	7,0	1,6	4,04	2,95	5,00	3,03	253

water temperature ( $T_w$ ), we also tested the sensitivity of the model when considering that  $T_w$  is equal to the air daily mean average temperature ( $T_{\text{air}}$ ). Finally, we tested for the uncertainties concerning the definition of the LMWL. For the reference scenario, the LMWL was estimated using an ordinary least square regression (OLSR). For the sensitivity analysis, we estimated the LMWL via a precipitation amount weighted least square regression (PWLSR), which was developed by Hughes and Crawford (2012). By doing so, recalculation of  $\delta_{\text{Is}}$ ,  $\delta_{\text{G}}$  was needed, as they were both assumed to plot on the LMWL (see Sect. 3.3.2). The results of this sensitivity analysis are listed in Table 2.



The model was found to be highly sensitive to the uncertainties associated with  $\delta_{Is}$ ,  $\delta_G$  and  $E$  and less importantly to  $\delta_A$  and  $T_w$ . Negligible to slight change on the modelled  $\delta_L$  was found when considering the uncertainties for  $V$ ,  $RH$ ,  $T$ ,  $U$ ,  $P$  and  $Rs$ . As expected, the value of  $\delta_{Is}$  is affecting the modelled  $\delta_L$  exclusively during springtime (i.e., the period of hydraulic connection with Lake DM). Similarly, the value of  $\delta_G$  and  $E$  particularly influence the modelled  $\delta_L$  from late summer to early winter. This is due to the fact that  $Q$  and  $E$  are the dominant fluxes during this period. When considering that  $T_w$  is equal to  $T_{air}$ , despite the significantly different maximum and minimum values for  $Q$ , the mean  $Q$  was relatively similar to the reference scenario and only small change for  $t_f$  was found. Finally, the model is highly sensitive to the uncertainties associated with the LMWL, since a translation of the LMWL implies an enrichment or depletion of both the  $\delta_{Is}$ ,  $\delta_G$  at the same time.

## 5 Discussion

### 5.1 Importance of groundwater on the annual lake budget

The water mass balance of Lake A from February 9, 2017 to January 25, 2018 is summarized in Table 3. The difference between the sum of the inputs ( $1.73 \times 10^7 \text{ m}^3$ ) and outputs ( $1.72 \times 10^7 \text{ m}^3$ ) corresponds to the lake volume difference ( $1.48 \times 10^5 \text{ m}^3$ ) between the start and the end of the model run. Groundwater ( $I_G$ ) and surface water ( $I_s$ ) account for 71 % and 28 % of the total water inputs to Lake A, respectively. Thus, it appears that the annual dynamic of Lake A is dominated by groundwater inputs, despite the intensity of the flooding event during springtime. Precipitation is contributing 1% of the total annual inputs and evaporation only accounts for 2% of the total annual outputs. Although the establishment of a hydraulic connection between Lake DM and Lake A is a recurring yearly hydrological process, it is important to note that the magnitude and duration of the flooding event of 2017 was particularly important and, thus, impacted more strongly the dynamic of Lake A in comparison to other years.

**Table 3. Water mass balance of Lake A for the reference scenario A. The difference between the sum of the inputs and outputs corresponds to the lake volume difference over the study period.**

Inputs	Volume ( $\text{m}^3$ )	Outputs	Volume ( $\text{m}^3$ )
Precipitation	$2.32 \times 10^5$	Evaporation	$4.04 \times 10^5$
Surface water (as flood-water)	$4.82 \times 10^6$	Groundwater and surface water	$1.68 \times 10^7$
Groundwater	$1.22 \times 10^7$		
Total	$1.73 \times 10^7$	Total	$1.72 \times 10^7$

Little information was available to constrain the modelled isotopic composition of the lake during springtime (see Fig. 4). In this perspective, a second scenario, for which the isotopic composition of the lake underwent a more important depletion due to the flood-water inputs during springtime, was also considered. The results of the sensitivity analysis and the water mass



balance for this second scenario are available in Table C1 and Table C2 of Appendix C. These two scenarios will be further referred to as reference scenarios A and B, respectively.

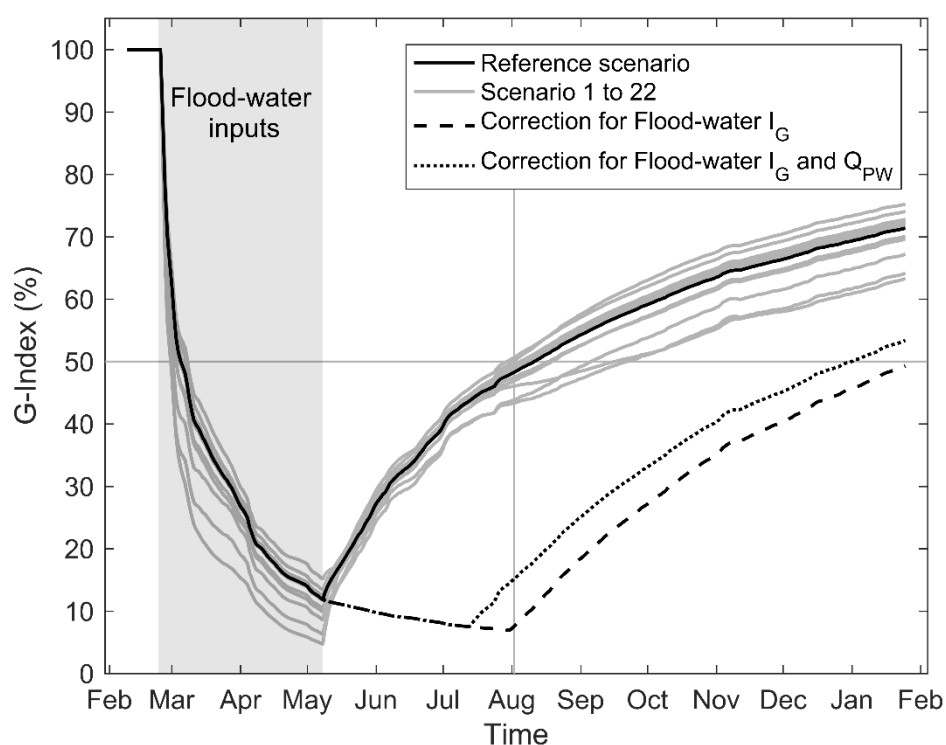
## 5.2 Temporal variability of the hydrological processes

The water balance presented in Table 3 provides an overview of the relative importance of the hydrological processes at Lake A on an annual timescale. As the surface water inputs (as flood-water) only occurred during springtime at Lake A, it is also important to decipher the temporal variability of the water fluxes. The dependence of a lake on groundwater can be quantified via the G-Index, which is the ratio of cumulative groundwater inputs to the cumulative total inputs (Isokangas et al., 2015). Figure 7 shows the temporal evolution of the G-Index from February 9, 2017 to January 25, 2018 for the reference scenario (see solid black line in Fig. 7) and all other scenarios considered in the sensitivity analysis (see solid grey lines in Fig. 7). Note that this G-Index is used to understand the relative importance of groundwater inputs over the studied period and does not consider the initial state of the lake. In early February, the G-Index is 100 %, since no surface water inputs ( $I_s$ ) or precipitation ( $P$ ) had yet contributed to the water balance. During the flood-water input period (see grey shaded area), the G-Index rapidly decreased and reached 12 % on May 8, 2017 (for the reference scenario). A gradual increase of the G-Index is then computed for the rest of the study period. On January 25, 2018, the G-Index is 71 % and is likely more representative of annual conditions. Despite the sensitivity of the model to the input parameters, all scenarios yielded similar results. The G-Index ranged from 62 % to 75 % on an annual timescale for the different scenarios (see solid grey lines in Fig. 7).

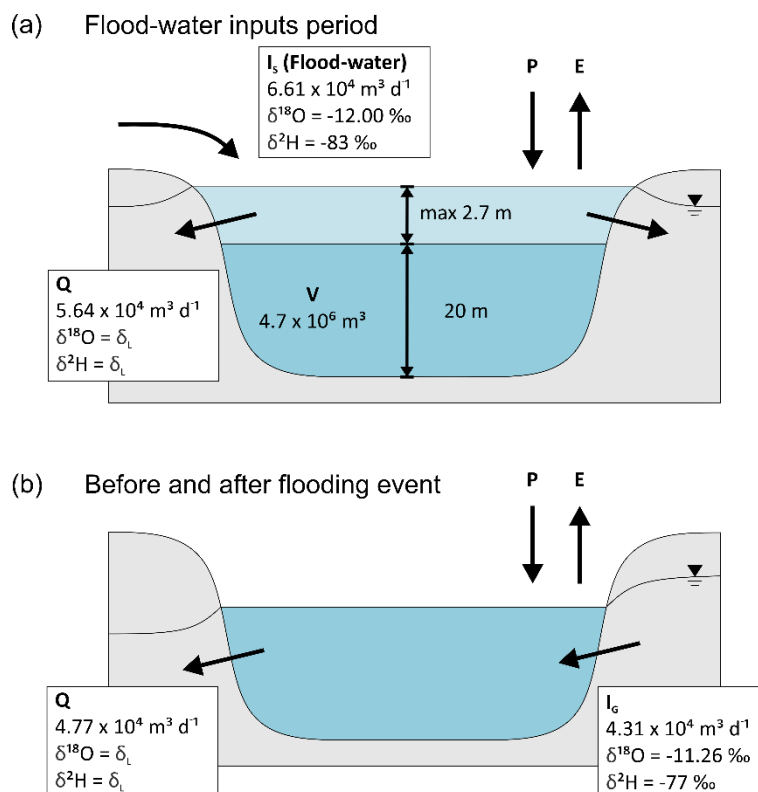
The isotopic mass balance model revealed it was necessary to allow for significant groundwater outflow from Lake A during springtime to correctly reproduce the observed  $\delta_L$ . In fact, the high surface water elevation of Lake A during springtime resulted in hydraulic gradients that forced lake water to infiltrate toward the aquifer and induce local recharge (see Fig. 8). During the flood-water input period, the total output volume from Lake A was  $4.12 \times 10^6 \text{ m}^3$ , representing 85 % of the surface water input. An important volume of flood-derived water could thus be stored in the aquifer in spring and discharged back to the lake during summertime, as its surface elevation decreased. Hence, the groundwater inputs to Lake A following the flooding event were likely corresponding to flood-derived surface water. By neglecting losses via abstraction from nearby pumping wells and/or other processes, we estimate recently recharged groundwater to represent up to 34 % of the total annual groundwater inputs. This scenario is also depicted in Fig. 7 (see dashed black line). In this hypothetical scenario, the temporal evolution of G-Index differs from the reference case. As surface water inputs were transferred to aquifer storage during springtime and discharged back to Lake A in summertime, we observe a temporal translation of the minimum G-Index, suggesting that the flood-water inputs impacted Lake A until early August (see vertical line in Fig. 7). However, part of the infiltrated Flood-water could have been pumped by the pumping wells between Lake A and Lake B. Assuming that from late February the total pumping rate corresponds to flood-derived surface water, the evolution of the computed G-Index suggests that Lake A could have been affected by the flood-water inputs until mid-July (see dotted black line in Fig. 7). In this perspective, Lake A is susceptible to flood-derived pollution during an extended period after the flooding event, as flood-derived surface water fluxes remain the main water input to the water budget until mid-July. Since these flood-water



inputs originate from Lake DM, this result suggests that water quality of Lake A is susceptible to changes in water quality of  
 470 Lake DM and the entire DM watershed. This highlights the need for protection and management of surface water resources  
 beyond local areas to the regional scale. Such considerations are important when assessing sensitivity of the water supply  
 system to surface water pollution (further discussed in next subsection).



475 **Figure 7. Evolution of the G-Index from February 9, 2017 to January 25, 2018 for the reference scenario (solid black line), for the  
 scenarios 1 to 22 assessed in the sensitivity analysis (solid grey lines) and for a hypothetical scenario for which the outputs from  
 Lake A during the flood-water inputs period are stored in the aquifer and discharged back into Lake A during summertime  
 (dotted black line). The grey shaded area corresponds to the flood-water input period.**



480 **Figure 8. Schematic representation of the hydrological processes at Lake A, (a) during the flood-water input period, and (b) during the rest of the hydrological year. Inputs include precipitation (P), surface water (Is) and groundwater (Ig) while outputs include evaporation (E) and surface and groundwater outflow (Q).**

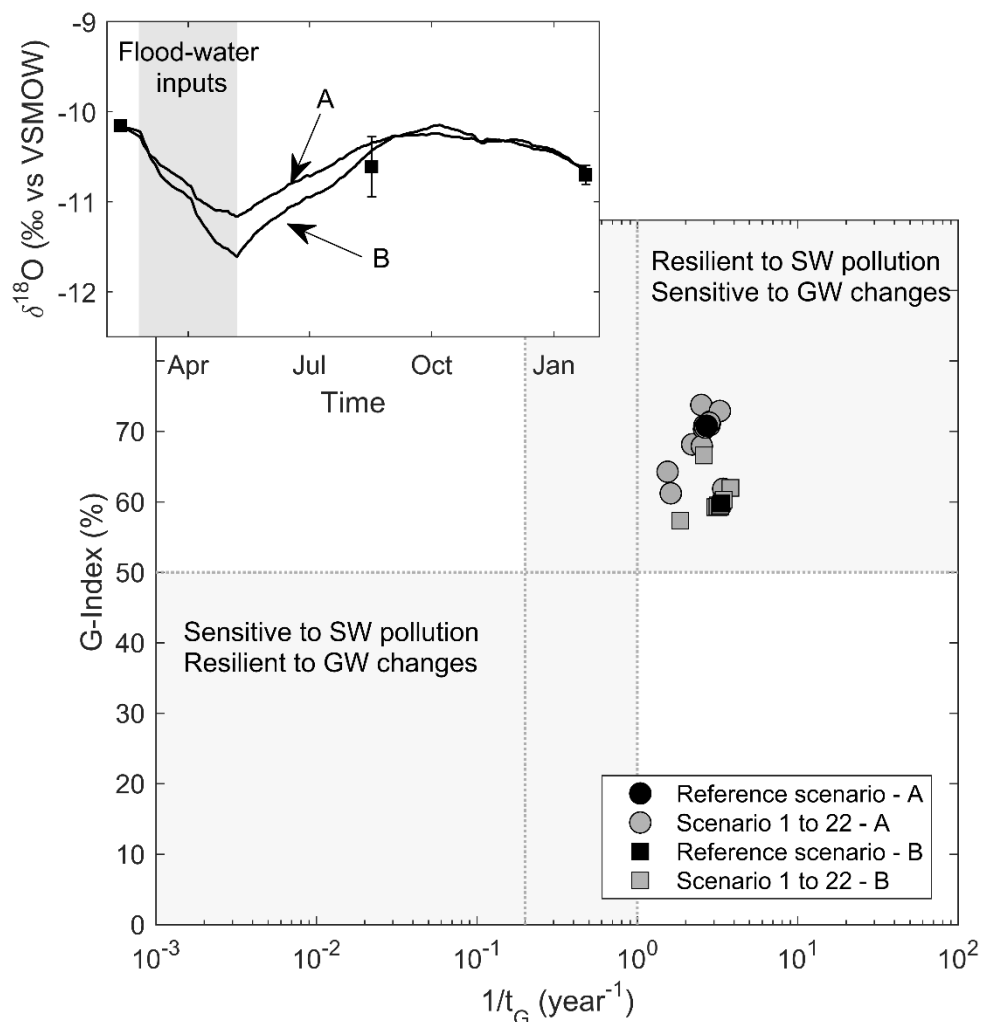
### 5.3 Resilience of Lake A to surface water pollution

The impact of a perturbation to a lake is not only dependent on the relative importance of water budget fluxes, but also on the residence time of water in the lake (Arnoux et al., 2017a). The mean flushing time by groundwater ( $t_G$ ) can be described as Eq. (13):

$$t_f = V/I_G \quad (13)$$

where  $V$  is the lake volume and  $I_G$  is the groundwater inflow rate. Figure 9 illustrates the relationship between the G-Index and  $1/t_f$  for the reference scenarios A and B and all the corresponding scenarios assessed in the sensitivity analysis. For the reference scenarios A and B,  $t_f$  values are 0.370 year and 0.299 year (or 135 days and 109 days), respectively. Thus, Lake A appears to be resilient to surface water pollution on an annual time scale, as it is characterized by high G-Index and  $1/t_f$  values (Arnoux et al., 2017a). The same interpretation applies for all scenarios evaluated, which strengthens the validity of our assumptions for the development of the isotopic mass balance model.





495 **Figure 9. Resilience of Lake A to surface water (SW) pollution, and sensitivity to groundwater (GW) quantity and quality changes. G-Index is the ratio of groundwater inputs to total inputs and  $t_G$  is the mean flushing time by groundwater. The reference scenario (black circle) is plotted along with the corresponding 22 scenarios from the sensitivity analysis (grey circles). A similar case, for which the isotopic composition of the lake underwent a more important depletion due to flood-water inputs is also plotted for comparison purpose (black and grey squares). This representation is adapted from (Arnoux et al., 2017a).**

500 Globally, future climate change scenarios are predicting changes in precipitation and climate extremes, including floods and droughts (Salinger, 2005). Studies concerning the hydrological response to future climate scenarios in Quebec, Canada have reported expected increases in water levels (Roy et al., 2001), earlier spring peak flows and overall increases in discharge (Dibike and Coulibaly, 2005) with the exception of summertime when discharge is expected to increase (Minville et al., 2008). These hydrological responses could result in floods of longer duration and higher intensity (Aissia et al., 2012) and

505 with more pronounced droughts (Wheaton et al., 2007). Such changes could directly affect the dynamics of Lake A. If flooding becomes more prevalent, enhanced flood-water input to Lake A would likely occur and recharge would be



increased during springtime. In this case, the surface water inputs from floods would buffer the sensitivity of Lake A to groundwater quality changes originating from its watershed. On the other hand, if floods become less important and/or less frequent, we can expect that the water quality of Lake A would be more dependent on regional groundwater quality.

## 510 6 Conclusions

In this study, we develop a volume-dependent transient isotopic mass balance model, assuming well-mixed conditions, in order to better understand the dynamics of the hydrological processes at a flood-affected lake in southern Canada. A yearly recurrent hydraulic connection allows for flood-water inputs from Lake DM to Lake A during springtime. These surface water inputs are marked by snowmelt waters which are characteristically depleted in heavy isotopes. Quantification of flood-  
 515 water inputs was done by adjusting minimum and maximum values for surface water and groundwater outflows from the lake to best-fit the observed depth-average lake isotopic compositions.

The isotopic mass balance model revealed that groundwater and surface water inputs account for 71 % and 28 %, respectively, of the total annual water inputs to Lake A, which demonstrates the importance of groundwater inputs to the annual water budget. Due to uncertainties associated with the input parameters in the model and the lack of data during  
 520 springtime, various scenarios were analyzed and helped strengthen our overall interpretations. All scenarios yielded similar results and suggested that Lake A is resilient to surface water pollution but may be sensitive to groundwater quantity and quality changes. However, there is a likelihood that the resilience to surface water pollution is lower from April to August, as important water inputs originating from Lake DM contribute to the water balance. In fact, during springtime, the hydraulic conditions allowed for flood-water inputs from Lake DM to Lake A at a mean rate of  $6.61 \times 10^4 \text{ m}^3 \text{ d}^{-1}$ , with a total flood-  
 525 water volume of  $4.82 \times 10^6 \text{ m}^3$  (i.e., 100 % of the initial lake's volume). Meanwhile, high surface water elevation of Lake A during springtime resulted in a hydraulic gradient which forced lake water to infiltrate toward the aquifer and induce local recharge. An important volume of flood-derived surface water could thus be stored within the aquifer in spring and discharged back to the lake during summertime, as its surface elevation decreased. This suggests that the surface water fluxes between Lake DM and Lake A do not only have an impact on the dynamic of Lake A during springtime but also  
 530 significantly influence the annual water budget. This finding provides the basis for speculation concerning the impact of climate change on the water quality of Lake A. If the importance of floods increases, more flood-water inputs to Lake A can be expected during springtime causing increased recharge. In this case, the surface water inputs from floods would buffer the sensitivity of Lake A to groundwater quality changes in its watershed. On the other hand, if floods become less important and/or less frequent, we can expect that the water quality of Lake A may become more dependent on regional groundwater  
 535 quality. From a global perspective, this knowledge is useful for establishing regional-scale management strategies for maintaining lake water quality.

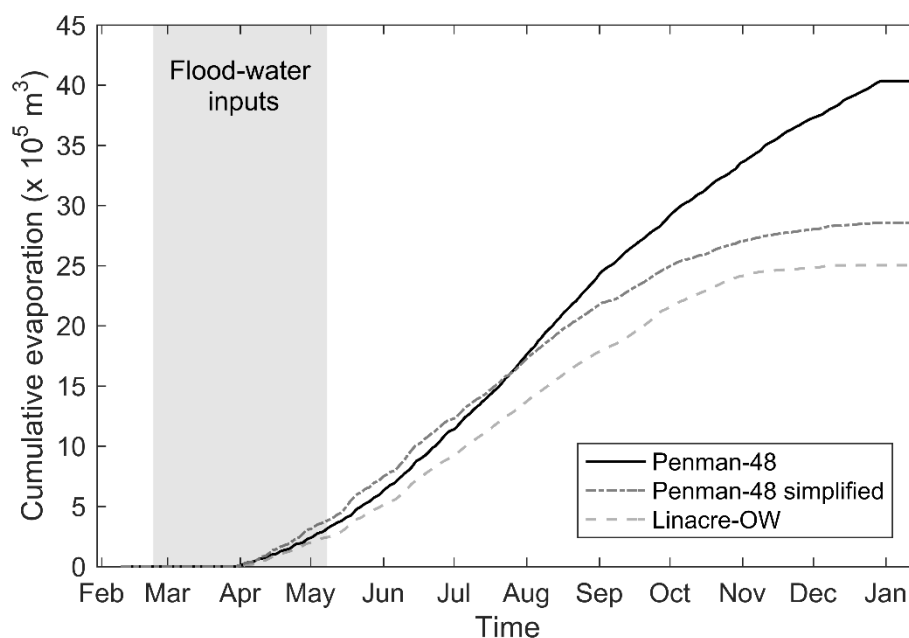
To improve upon this work, better characterization of the potential spatial and temporal variability of the groundwater and flood-water isotopic and geochemical signatures would be needed, as the model was found to be sensitive to these



parameters. Moreover, as climate change and/or human activities may affect the magnitude and/or duration of the yearly  
 540 recurrent hydraulic connection between Lake DM and Lake A, some specific field campaigns are recommended that target  
 improved understanding of the sensitivity of the lake to future changes in quantity and quality of groundwater in the  
 watershed.

## Appendix A

See Figure A1



545

**Figure A1.** Cumulative evaporative fluxes from Lake A via the Penman-48, Penman-48 simplified method (Valiantzas, 2006) and Linacre-OW (Linacre, 1977) methods.

## Appendix B

Figure B1 shows the daily average air temperature and the observed and estimated water surface temperatures. During  
 550 springtime, the air and water temperatures are relatively similar, but diverge from July 2017 to January 2018. This  
 discrepancy is explained by heat storage. Hence, in late summer and autumn, the water surface temperature is higher than the  
 air temperature. This has an impact on the estimation of  $E$  (see Eq.11) and  $\delta E$  (see Eq.3).

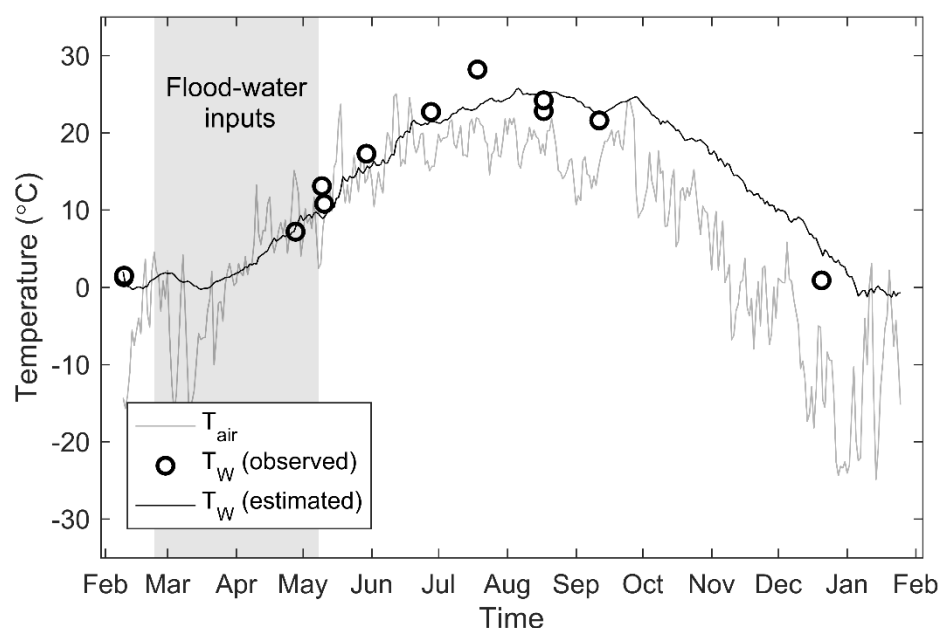


**Figure B1.** Temporal evolution of air temperature ( $T_{air}$ ) and water temperature ( $T_w$ ) at Lake A. Discrete observed  $T_w$  and continuous estimated  $T_w$  are represented by hollow blue circles and solid blue line, respectively.

## Appendix C

See Table C1 and Table C2.

**Table C1.** Water mass balance of Lake A for the reference scenario B. The difference between the sum of the inputs and outputs corresponds to the lake volume difference over the study period.

Inputs	Volumes ( $m^3$ )	Outputs	Volumes ( $m^3$ )
Precipitation	$2.32 \times 10^5$	Evaporation	$4.04 \times 10^5$
Surface water (as flood-water)	$9.96 \times 10^6$	Groundwater and surface water	$2.48 \times 10^7$
Groundwater	$1.51 \times 10^7$		
Total	$2.53 \times 10^7$	Total	$2.52 \times 10^7$



**Table C2. Sensitivity analysis on the input parameters of the isotopic mass balance model for the reference scenario B. Q is the output flux from Lake A, I the input flux and  $t_f$  the mean flushing time by groundwater.**

Scenario		Maximum Q ( $\times 10^4 \text{ m}^3 \text{ d}^{-1}$ )	Minimum Q ( $\text{m}^3 \text{ d}^{-1}$ )	Mean Q		Mean I		Tf = V/IG (days)
				Flooding ( $\times 10^4 \text{ m}^3 \text{ d}^{-1}$ )	Annual ( $\times 10^4 \text{ m}^3 \text{ d}^{-1}$ )	Flooding ( $\times 10^4 \text{ m}^3 \text{ d}^{-1}$ )	Annual ( $\times 10^4 \text{ m}^3 \text{ d}^{-1}$ )	
B	Reference	28,0	1,0E+03	12,68	7,07	13,65	7,16	135
B01	V + 3% (slope 30°)	28,0	1,0E+01	12,63	6,99	13,59	7,07	140
B02	V - 8% (slope 20°)	26,0	1,0E+01	11,73	6,49	12,69	6,57	129
B03	$\delta_{\text{Is}}^{18}\text{O} + 0.5 \text{ ‰}$ $\delta_{\text{Is}}^2\text{H} + 4 \text{ ‰}$			Not possible to fit data				
B04	$\delta_{\text{Is}}^{18}\text{O} - 0.5 \text{ ‰}$ $\delta_{\text{Is}}^2\text{H} - 4 \text{ ‰}$	12,0	2,5E+04	6,78	4,87	7,75	4,95	150
B05	$\delta_{\text{G}}^{18}\text{O} + 0.5 \text{ ‰}$ $\delta_{\text{G}}^2\text{H} + 4 \text{ ‰}$			Not possible to fit data				
B06	$\delta_{\text{G}}^{18}\text{O} - 0.5 \text{ ‰}$ $\delta_{\text{G}}^2\text{H} - 4 \text{ ‰}$			Not possible to fit data				
B07	$\delta_{\text{A}}$ minimum	26,0	1,0E+01	11,73	6,49	12,69	6,57	147
B08	$\delta_{\text{A}}$ maximum			Negligible change				
B09	E + 20%	28,0	1,0E+04	13,18	7,74	14,15	7,84	110
B10	E - 20%	27,0	1,0E+01	12,18	6,74	13,13	6,80	156
B11	RH + 10%			Negligible change				
B12	RH - 10%							
B13	T + 10%			Negligible change				
B14	T - 10%							
B15	U + 10%	28,0	2,0E+03	12,74	7,14	13,70	7,23	130
B16	U - 10%	28,0	1,0E+01	12,63	6,99	13,59	7,08	137
B17	P + 10%			Negligible change				
B18	P - 10%							
B19	$T_{\text{w}} = T_{\text{air}}$	28,0	1,0E+01	12,63	6,99	13,60	7,05	145
B20	$R_{\text{s}} + 10\%$	28,0	3,0E+03	12,79	7,22	13,76	7,31	125
B21	$R_{\text{s}} - 10\%$	28,0	1,0E+01	12,63	6,99	13,59	7,07	146
B22	LMWL (PWLSR method)	16,0	1,0E+01	7,22	4,00	8,18	4,08	253



## Author contribution

570 JMD: Conceptualization, Data curation, Investigation, Methodology, Visualization, Roles/Writing - original draft. FB: Conceptualization, Methodology, Supervision, Writing - review & editing. PB: Conceptualization, Funding acquisition, Project administration, Supervision, Writing - review & editing. JG: Methodology, Writing - review & editing.

## Competing interests

The authors declare that they have no conflict of interest.

## 575 Acknowledgements

This research was funded by NSERC, grant numbers CRSNG-RDCPJ: 523095-17 and CRSNG-RGPIN-2016-06780. The authors are grateful to the Town and G. Rybicki to allow access and water sampling on their property. Thanks to the students (M. Patenaude, T. Crouzal, R.-A. Farley, just to name a few) who participated in the fieldwork. We also gratefully acknowledge J.-F. Helie and M. Tcaci from Geotop-UQAM and M. Leduc and J. Leroy from the Laboratoire de géochimie  
 580 de Polytechnique Montréal.

## References

- Ageos: Alimentation en eau potable: Demande d'autorisation en vertu de l'Article 31 du Règlement sur le captage des eaux souterraines : Rapport d'expertise hydrogéologique AGEOS, Brossard, QC2010-723, volume 1 de 2, 2010.
- 585 Aissia, M. A. B., Chebana, F., Ouarda, T. B. M. J., Roy, L., Desrochers, G., Chartier, I., and Robichaud, É.: Multivariate analysis of flood characteristics in a climate change context of the watershed of the Baskatong reservoir, Province of Québec, Canada, *Hydrological Processes*, 26, 130-142, 10.1002/hyp.8117, 2012.
- Arnoux, M., Barbecot, F., Gibert-Brunet, E., Gibson, J., Rosa, E., Noret, A., and Monvoisin, G.: Geochemical and isotopic mass balances of kettle lakes in southern Quebec (Canada) as tools to document variations in groundwater quantity and quality, *Environmental Earth Sciences*, 76, 106, 10.1007/s12665-017-6410-6, 2017a.
- 590 Arnoux, M., Gibert-Brunet, E., Barbecot, F., Guillon, S., Gibson, J., and Noret, A.: Interactions between groundwater and seasonally ice-covered lakes: Using water stable isotopes and radon-222 multilayer mass balance models, *Hydrological Processes*, 31, 2566-2581, 10.1002/hyp.11206, 2017b.
- Bocanegra, E., Quiroz Londoño, O. M., Martínez, D. E., and Romanelli, A.: Quantification of the water balance and hydrogeological processes of groundwater-lake interactions in the Pampa Plain, Argentina, *Environmental Earth Sciences*, 68, 2347-2357, 10.1007/s12665-012-1916-4, 2013.
- 595 Brock, B. E., Wolfe, B. B., and Edwards, T. W. D.: Characterizing the Hydrology of Shallow Floodplain Lakes in the Slave River Delta, NWT, Canada, Using Water Isotope Tracers, *Arctic, Antarctic, and Alpine Research*, 39, 388-401, 10.1657/1523-0430(06-026)[BROCK]2.0.CO;2, 2007.
- Brooks, J. R., Gibson, J. J., Birks, S. J., Weber, M. H., Rodecap, K. D., and Stoddard, J. L.: Stable isotope estimates of evaporation : inflow and water residence time for lakes across the United States as a tool for national lake water quality assessments, *Limnology and Oceanography*, 59, 2150-2165, 10.4319/lo.2014.59.6.2150, 2014.
- 600 Craig, H., and Gordon, L. I.: Deuterium and oxygen 18 variations in the ocean and the marine atmosphere, in: *Stable isotopes in oceanographic studies and paleotemperatures*, edited by: Tongiorgi, E., Lab. Geologia Nucleare, Pisa, 9-130, 1965.
- 605 Cunha, D. G. F., Sabogal-Paz, L. P., and Dodds, W. K.: Land use influence on raw surface water quality and treatment costs for drinking supply in São Paulo State (Brazil), *Ecological Engineering*, 94, 516-524, 10.1016/j.ecoleng.2016.06.063, 2016.



- de Bruin, H. A. R.: Temperature and energy balance of a water reservoir determined from standard weather data of a land station, *Journal of Hydrology*, 59, 261-274, 10.1016/0022-1694(82)90091-9, 1982.
- Delpla, I., Jung, A. V., Baures, E., Clement, M., and Thomas, O.: Impacts of climate change on surface water quality in relation to drinking water production, *Environment International*, 35, 1225-1233, 10.1016/j.envint.2009.07.001, 2009.
- 610 Dibike, Y. B., and Coulibaly, P.: Hydrologic impact of climate change in the Saguenay watershed: comparison of downscaling methods and hydrologic models, *Journal of Hydrology*, 307, 145-163, 10.1016/j.jhydrol.2004.10.012, 2005.
- Edwards, T. W. D., Wolfe, B. B., Gibson, J. J., and Hammarlund, D.: Use of water isotope tracers in high latitude hydrology and paleohydrology, in: Long-term environmental change in Arctic and Antarctic Lakes, developments in paleoenvironmental research, edited by: Pienitz, R., Douglas, M., and Smol, J. P., Springer, Dordrecht, Netherlands, 187-207, 2004.
- 615 Gibson, J. J., Edwards, T. W. D., Bursey, G. G., and Prowse, T. D.: Estimating Evaporation Using Stable Isotopes: Quantitative Results and Sensitivity Analysis for Two Catchments in Northern Canada: Paper presented at the 9th Northern Res. Basin Symposium/Workshop (Whitehorse/Dawson/Inuvik, Canada - August 1992), *Hydrology Research*, 24, 79-94, 10.2166/nh.1993.0015, 1993.
- Gibson, J. J.: Short-term evaporation and water budget comparisons in shallow Arctic lakes using non-steady isotope mass balance, *Journal of Hydrology*, 264, 242-261, 10.1016/S0022-1694(02)00091-4, 2002.
- 620 Gibson, J. J., Birks, S. J., and Yi, Y.: Stable isotope mass balance of lakes: a contemporary perspective, *Quaternary Science Reviews*, 131, 316-328, 10.1016/j.quascirev.2015.04.013, 2015.
- Gibson, J. J., Birks, S. J., Yi, Y., Moncur, M. C., and McEachern, P. M.: Stable isotope mass balance of fifty lakes in central Alberta: Assessing the role of water balance parameters in determining trophic status and lake level, *Journal of Hydrology: Regional Studies*, 6, 13-25, 10.1016/j.ejrh.2016.01.034, 2016.
- 625 Gibson, J. J., Birks, S. J., Jeffries, D., and Yi, Y.: Regional trends in evaporation loss and water yield based on stable isotope mass balance of lakes: The Ontario Precambrian Shield surveys, *Journal of Hydrology*, 544, 500-510, 10.1016/j.jhydrol.2016.11.016, 2017.
- Gibson, J. J., Yi, Y., and Birks, S. J.: Isotopic tracing of hydrologic drivers including permafrost thaw status for lakes across Northeastern Alberta, Canada: A 16-year, 50-lake assessment, *Journal of Hydrology: Regional Studies*, 26, 100643, 10.1016/j.ejrh.2019.100643, 2019.
- 630 Gonfiantini, R.: Chapter 3 - ENVIRONMENTAL ISOTOPES IN LAKE STUDIES, in: *The Terrestrial Environment*, B, edited by: Fritz, P., and Fontes, J. C., Elsevier, Amsterdam, 113-168, 1986.
- Gran, G.: Determination of the equivalence point in potentiometric titrations. Part II, *Analyst*, 77, 661-671, 10.1039/AN9527700661, 1952.
- 635 Holtz, R. D., and Kovacs, W. D.: *An Introduction to Geotechnical Engineering*, Montreal, Canada, 832 pp., 1981.
- Horita, J., and Wesolowski, D. J.: Liquid-vapor fractionation of oxygen and hydrogen isotopes of water from the freezing to the critical temperature, *Geochimica et Cosmochimica Acta*, 58, 3425-3437, 10.1016/0016-7037(94)90096-5, 1994.
- Horita, J., Rozanski, K., and Cohen, S.: Isotope effects in the evaporation of water: a status report of the Craig-Gordon model, *Isotopes in Environmental and Health Studies*, 44, 23-49, 10.1080/10256010801887174, 2008.
- 640 Hughes, C. E., and Crawford, J.: A new precipitation weighted method for determining the meteoric water line for hydrological applications demonstrated using Australian and global GNIP data, *Journal of Hydrology*, 464-465, 344-351, 10.1016/j.jhydrol.2012.07.029, 2012.
- Hutchinson, G. E.: *A Treatise on Limnology*, John Wiley and Sons, New York, 1115 pp., 1957.
- Isokangas, E., Rozanski, K., Rossi, P. M., Ronkanen, A. K., and Kløve, B.: Quantifying groundwater dependence of a sub-polar lake cluster in Finland using an isotope mass balance approach, *Hydrol. Earth Syst. Sci.*, 19, 1247-1262, 10.5194/hess-19-1247-2015, 2015.
- 645 Jeppesen, E., Meerhoff, M., Davidson, T. A., Trolle, D., Sondergaard, M., Lauridsen, T. L., Beklioglu, M., Brucet Balmaña, S., Volta, P., and González-Bergonzoni, I.: Climate change impacts on lakes: an integrated ecological perspective based on a multi-faceted approach, with special focus on shallow lakes, 73, 88-111, 10.4081/jlimnol.2014.844, 2014.
- 650 Kløve, B., Ala-aho, P., Bertrand, G., Boukalova, Z., Ertürk, A., Goldscheider, N., Ilmonen, J., Karakaya, N., Kupfersberger, H., Kværner, J., Lundberg, A., Mileusnić, M., Moszczynska, A., Muotka, T., Preda, E., Rossi, P., Siergieiev, D., Šimek, J., Wachniew, P., Angheluta, V., and Widerlund, A.: Groundwater dependent ecosystems. Part I: Hydroecological status and trends, *Environmental Science & Policy*, 14, 770-781, 10.1016/j.envsci.2011.04.002, 2011.
- Lerner, D. N., and Harris, B.: The relationship between land use and groundwater resources and quality, *Land Use Policy*, 26, S265-S273, 10.1016/j.landusepol.2009.09.005, 2009.
- 655 Linacre, E. T.: A simple formula for estimating evaporation rates in various climates, using temperature data alone, *Agricultural Meteorology*, 18, 409-424, 10.1016/0002-1571(77)90007-3, 1977.
- Masse-Dufresne, J., Baudron, P., Barbecot, F., Patenaude, M., Pontoreau, C., Proteau-Bédard, F., Menou, M., Pasquier, P., Veuille, S., and Barbeau, B.: Anthropogenic and Meteorological Controls on the Origin and Quality of Water at a Bank Filtration Site in Canada, *Water*, 11, 2510, 10.3390/w11122510, 2019.
- 660





- McJannet, D. L., Webster, I. T., and Cook, F. J.: An area-dependent wind function for estimating open water evaporation using land-based meteorological data, *Environmental Modelling & Software*, 31, 76-83, 10.1016/j.envsoft.2011.11.017, 2012.
- Minville, M., Brissette, F., and Leconte, R.: Uncertainty of the impact of climate change on the hydrology of a nordic watershed, *Journal of Hydrology*, 358, 70-83, 10.1016/j.jhydrol.2008.05.033, 2008.
- 665 Mueller, H., Hamilton, D. P., and Doole, G. J.: Evaluating services and damage costs of degradation of a major lake ecosystem, *Ecosystem Services*, 22, 370-380, 10.1016/j.ecoser.2016.02.037, 2016.
- Petermann, E., Gibson, J. J., Knöller, K., Pannier, T., Weiß, H., and Schubert, M.: Determination of groundwater discharge rates and water residence time of groundwater-fed lakes by stable isotopes of water ( $^{18}\text{O}$ ,  $2\text{H}$ ) and radon ( $^{222}\text{Rn}$ ) mass balances, *Hydrological Processes*, 32, 805-816, 10.1002/hyp.11456, 2018.
- 670 Rosa, E., Hillaire-Marcel, C., Hélie, J.-F., and Myre, A.: Processes governing the stable isotope composition of water in the St. Lawrence river system, Canada, *Isotopes in Environmental and Health Studies*, 52, 370-379, 10.1080/10256016.2015.1135138, 2016.
- Rosenberry, D. O., Lewandowski, J., Meinikmann, K., and Nützmann, G.: Groundwater - the disregarded component in lake water and nutrient budgets. Part 1: effects of groundwater on hydrology, *Hydrological Processes*, 29, 2895-2921, 10.1002/hyp.10403, 2015.
- Roy, L., Leconte, R., Brissette, F. P., and Marche, C.: The impact of climate change on seasonal floods of a southern Quebec River Basin, *Hydrological Processes*, 15, 3167-3179, 10.1002/hyp.323, 2001.
- 675 Sacks, L. A., Lee, T. M., and Swancar, A.: The suitability of a simplified isotope-balance approach to quantify transient groundwater-lake interactions over a decade with climatic extremes, *Journal of Hydrology*, 519, 3042-3053, 10.1016/j.jhydrol.2013.12.012, 2014.
- Salinger, M. J.: Climate Variability and Change: Past, Present and Future – An Overview, *Climatic Change*, 70, 9-29, 10.1007/s10584-005-5936-x, 2005.
- 680 Scanlon, B. R., Reedy, R. C., Stonestrom, D. A., Prudic, D. E., and Dennehy, K. F.: Impact of land use and land cover change on groundwater recharge and quality in the southwestern US, *Global Change Biology*, 11, 1577-1593, 10.1111/j.1365-2486.2005.01026.x, 2005.
- Schallenberg, M., de Winton, M. D., Verburg, P., Kelly, D. J., Hamill, K. D., and Hamilton, D. P.: Ecosystem services of lakes, in: *Ecosystem services in New Zealand: conditions and trends*. Manaaki Whenua Press, Lincoln, edited by: Dymond, J. R., Manaaki Whenua Press, Lincoln, New Zealand, 203-225, 2013.
- 685 Stets, E. G., Winter, T. C., Rosenberry, D. O., and Striegl, R. G.: Quantification of surface water and groundwater flows to open- and closed-basin lakes in a headwaters watershed using a descriptive oxygen stable isotope model, *Water Resources Research*, 46, 10.1029/2009WR007793, 2010.
- Turner, K. W., Wolfe, B. B., and Edwards, T. W. D.: Characterizing the role of hydrological processes on lake water balances in the Old Crow Flats, Yukon Territory, Canada, using water isotope tracers, *Journal of Hydrology*, 386, 103-117, 10.1016/j.jhydrol.2010.03.012, 2010.
- 690 Valiantzas, J. D.: Simplified versions for the Penman evaporation equation using routine weather data, *Journal of Hydrology*, 331, 690-702, 10.1016/j.jhydrol.2006.06.012, 2006.
- Walsh, J. R., Carpenter, S. R., and Vander Zanden, M. J.: Invasive species triggers a massive loss of ecosystem services through a trophic cascade, *Proceedings of the National Academy of Sciences*, 113, 4081, 10.1073/pnas.1600366113, 2016.
- 695 Wetzel, R. G.: *Limnology*, W. B. Saunders Co., Philadelphia, London, and Toronto, 743 pp., 1975.
- Wolfe, B. B., Karst-Riddoch, T. L., Hall, R. I., Edwards, T. W. D., English, M. C., Palmini, R., McGowan, S., Leavitt, P. R., and Vardy, S. R.: Classification of hydrological regimes of northern floodplain basins (Peace–Athabasca Delta, Canada) from analysis of stable isotopes ( $\delta^{18}\text{O}$ ,  $\delta^2\text{H}$ ) and water chemistry, *Hydrological Processes*, 21, 151-168, 10.1002/hyp.6229, 2007.
- 700 Zimmermann, U.: Determination by stable isotopes of underground inflow and outflow and evaporation of young artificial groundwater lakes, in: *Isotopes in lakes studies*, IAEA, Vienna, Austria, 87-94, 1979.